The Meteorological Magazine

February 1992

Retirement of Sir John Houghton
Models and images
Results from infrared and microwave experiments
Direction of gusts and lulls
Winter of 1990/91
Noctilucent clouds 1990

DUPLICATE JOURNALS

National Meteorological Library
FitzRoy Road, Exeter, Devon. EX1 3PB

HMSO

Met.O.1004 Vol. 121 No. 1435

© Crown copyright 1992.
Applications for reproduction should be made to HMSO.

First published 1991

HMSO publications are available from:

HMSO Publications Centre
(Mail and telephone only)
PO Box 276, London, SW8 5DT
Telephone orders 071-873 9090
General enquiries 071-873 0011
(queuing system in operation for both numbers)

HMSO Bookshops
49 High Holborn, London, WC1V 6HB 071-873 0011 (counter service only)
258 Broad Street, Birmingham, B1 2HE 021-643 3740
Southey House, 33 Wine Street, Bristol, BS1 2BQ (0272) 264306
9–21 Princess Street, Manchester, M60 8AS 061-834 7201
80 Chichester Street, Belfast, BT1 4JY (0232) 238451
71 Lothian Road, Edinburgh, EH3 9AZ 031-228 4181

HMSO's Accredited Agents
(see Yellow Pages)

and through good booksellers

The
Meteorological Magazine

February 1992
Vol. 121 No. 1435

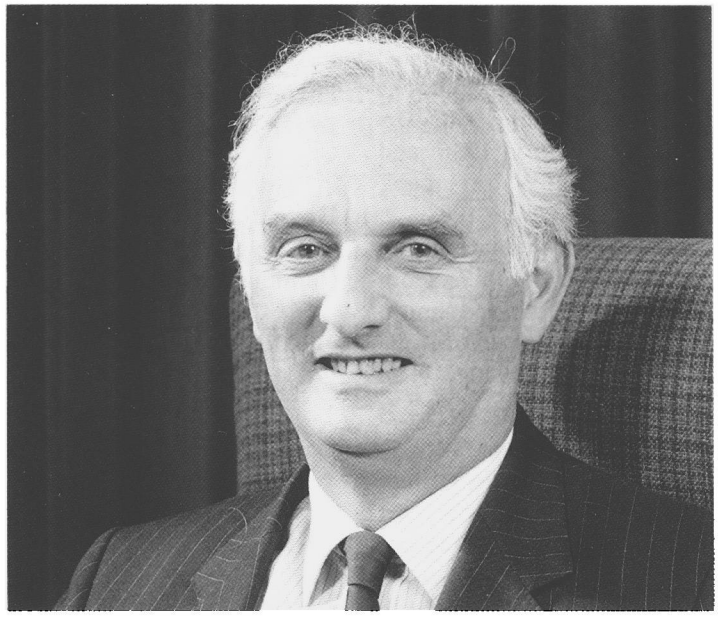

Retirement of Sir John Houghton

Sir John Houghton, CBE, FRS, took up his appointment as Director-General of the Meteorological Office on 1 October 1983, prior to which he was Deputy Director of the Rutherford Appleton Laboratory, SERC.

Born in 1931, Sir John was educated at Rhyl Grammar School and was a scholar at Jesus College, Oxford, where he took a double first in mathematics and physics. A Research Student in the Department of Meteorology, Clarendon Laboratory, from 1951–54, he took his D. Phil. in 1955. He was a Research Fellow at the Royal Aircraft Establishment, Farnborough, before returning to Oxford in 1958 as Lecturer in Atmospheric Physics. In 1962 he was appointed Reader and became Professor in 1976. Official Fellow and Tutor in Physics at Jesus from 1960–73, he became Professorial Fellow in 1973 and Honorary Fellow in 1983. He spent a term in 1969 as Visiting Professor at the University of California, Los Angeles. In 1979 Sir John was seconded from Oxford University to the Science and Engineering Research Council to be Director of the Appleton Laboratory during its move from Slough to Chilton to merge with the Rutherford Laboratory, adding to that laboratory a substantial expertise in space science and applications.

Elected Fellow of the Royal Society in 1972, Sir John is also Fellow of the Institute of Physics, Fellow of the Royal Meteorological Society (President 1976–78) and was awarded the Royal Meteorological Society's Darton Prize 1954, Buchan Prize 1966 and Symons Gold Medal 1991, the Charles Chree Medal of the Institute of Physics 1979, and the Glazebrook Medal 1990. He shared the Rank Prize for Opto-Electronics in 1988 with F.W. Taylor, C.D. Rogers and G.D. Peskett and in 1989 gave the Royal Society's Bakerian Prize Lecture. He is also a Fellow of the Optical Society of America and a Member of the American Meteorological Society and the American Geophysical Union. Between 1981 and early 1984 Sir John was Chairman of the Joint Scientific Committee for World Climate Research Programmes. Since 1983 he has been a member of the Executive Committee of the World Meteorological Organization (WMO) and from 1987 to 1991 was one of WMO's Vice-Presidents.

In 1988 Sir John was appointed as Chairman of the Scientific Assessment Working Group of the Intergovernmental Panel On Climate Change jointly set up by WMO and the UN Environment Programme. That Working Group produced a Report in September 1990 on the likely change in climate during the coming century due to the increasing release of greenhouse gases into the atmosphere. The Report has been very well received and as a result has had a substantial influence on the development of government policy in the United Kingdom and elsewhere concerning climate change.

In 1990 Sir John became the first Chief Executive of the Meteorological Office as it achieved Agency status within the Ministry of Defence. Under his guidance the year has been marked by commercial success and improvements in the range and quality of services.

Sir John has authored or co-authored several books — *Infra Red Physics* (with S.D. Smith) 1966, *The Physics of Atmospheres* 1977 (2nd edition 1986) and *Remote Sensing of Atmospheres* (with F.W. Taylor and C.D. Rogers) 1984 and *Does God Play Dice?* 1988.

Sir John is well known internationally for his outstanding research in remote sensing of the atmosphere from space. In co-operation with Professor Desmond Smith, he developed the Selective Chopper Radiometer for the Nimbus 4 and 5 satellites in the early 1970s — an instrument which sensed remotely the atmospheric temperature structure up to about 50 km altitude. Further developments by the group at Oxford led by Sir John, namely the Pressure Modulator Radiometer flown on Nimbus 6 in 1975 and the Stratospheric and Mesospheric Sounder flown on Nimbus 7 in 1978, enabled the temperature structure and the distribution of some minor constituents up to about 90 km altitude to be observed. These instruments provided, for the first time, global information of the structure of the stratosphere and mesosphere and have played a large part in enabling a detailed study of the radiation, dynamics and chemistry of the whole atmosphere to be pursued. Sir John also co-operated with Professor Fred Taylor, then at the Jet Propulsion Laboratory, in an instrument for the Pioneer Venus Orbiter in 1978. His interests in space activities continue — he is currently a member of the Board of the British National Space Centre.

In the Queen's Birthday Honours of 1991 Dr Houghton received the accolade of Knight Bachelor. In October 1991 he was appointed a member of the Royal Commission on Environmental Pollution.

Sir John is married, with two children and one grandchild. He lives in Begbroke, Oxon.

P. Ryder

The following articles are intended as a review of, and lead into, the main article. They represent an innovation which is part of the proposed expansion of the magazine.

Numerical weather prediction

Nina Morgan
Science writer

How is it possible to summarize the nature of weather systems, with all their quirks and complications, in a mathematical model? This is the problem those who work on numerical weather prediction (NWP) face daily – and not everyone views the problem in the same way.

1. Several models in use

There are a number of different NWP models currently in use around the world. For example, the

Meteorological Office in Bracknell, the European Centre for Medium-range Weather Forecasts in Shinfield, Reading in the United Kingdom, and the Japan Meteorological Agency all run different NWP models.

In the Bracknell Met. Office three models are run, a global area model, which covers the entire surface of the Earth and has a resolution of 20 levels and a grid spacing of 100 km; a limited area model covering Europe and the Atlantic, which has a resolution of 20 levels and grid points located 50 km apart; and the mesoscale model, covering only the United Kingdom and nearby areas on the continent, in which the grid points are 15 km apart and the resolution 32 levels.

The Japan Meteorological Agency run four models: a global model, with a resolution of 21 layers and a grid spacing of 110 km; an Asia model, with a resolution of 16 layers and a grid spacing of 75 km; a Japan model with a resolution of 19 layers and a grid spacing of 40 km; and a typhoon model, with a resolution of 8 layers and a grid spacing of 50 km.

All of the models are forced by the global model because they provide boundary and starting conditions for each of the higher-resolution models. Generally, the more localized the models, the higher the resolution. However, because higher-resolution models require a great deal of computer power to run, they are limited to a restricted area.

2. Navier–Stokes Equations

At the heart of each model are the Navier–Stokes equations, which describe the dynamics of fluid motion, and form the basis for describing flow in the atmosphere. Although the equations are the same, the models often differ in the approach taken to solving them.

There are two distinct methods in use — the grid-point method, used, for instance by the UK Met. Office in Bracknell, and the spectral model used, for example, by the Japan Meteorological Agency.

In the grid-point method the area being modelled is divided into a grid. The basic atmospheric variables are assigned values at each of the grid points, and values between the grid points are averaged.

In the spectral model, complex functions are used to describe the shape of flow in a given area. By applying a similar principle to the three-dimensional area of the model as that used in Fourier transforms for linear data, it is possible to describe conditions at any given point.

Although the spectral model is perhaps more difficult for outsiders to understand, it has some advantages. It more closely represents the wave nature of real atmospheric flow, preserving the speed and shape of individual components with different horizontal scales.

3. Physical parameters

Critical to all of the models are the physical process equations used to describe radiation, convection and turbulence in the atmosphere. These processes occur on scales which are smaller than can be resolved by the models.

The flexibility of the physics routines makes it possible to use the same model to predict weather in the tropics, where convection is very important, and at temperate latitudes, where cyclones and anticyclones dominate.

4. Keeping the models on track

The models are only able to predict a few days into the future with any degree of reliability — the current maximum limit is around 5 days. Errors in the initial variables and in the mathematical models mean that the predictions stray progressively from reality as time goes on.

To nudge the forecasts back into line, every observation which comes through the communications network is introduced into the model through an assimilation process. The model uses this information to continuously adjust its results. Usually the physics routines are the first to be altered because they contain more adjustable features. In general, the higher the resolution of the model being run, the greater the attempt made to incorporate information from satellites into the modelling process.

5. The future

NWP is central to any weather forecasting system, and its ultimate aims are to provide a more accurate representation of the weather than is presently possible. Improving the models and increasing the resolution by using bigger and better computers would go some way towards reaching this goal.

However, the greatest improvements will probably be due to improved observations collected from individual weather stations on the ground, geostationary satellites or aircraft. The human input into the models contributes as much to the accuracy of the predictions as do the supercomputers which run the models several times a day. By working together humans and computers can go along way towards untangling the complex weather maze and providing accurate forecasts.

(Information from Rick Rawlins and Akihide Segami)

Using satellite images

Nina Morgan
Science writer

1. Information from satellite images

Satellite imagery, which gives global coverage, has now surpassed point-data observations in the science of weather prediction. To trained interpreters, satellite and

radar images give a useful picture of the dynamic and physical processes going on in the atmosphere, and provide helpful clues as to the likely evolution of atmospheric systems.

Satellites provide a global view of the weather. As they orbit the Earth they record weather data at regular intervals to supplement data gathered on the ground. They are also able to gather information from those parts that ground-based weather stations do not reach — for example over the oceans — or places, such as much of the southern hemisphere, where weather stations are relatively thin on the ground.

The first weather satellite was launched in 1960. Now an array of geostationary and polar-orbiting satellites provide a continuous flow of information to forecasters and a constant stream of data to verify and update numerical weather prediction models.

In nowcasting, the very-short-term forecasting of weather, satellite and radar images are an essential aid in predicting relatively short-lived phenomena such as thunderstorms which may easily be missed by other types of observations. The images also provide data for use in longer-term forecasts, including the monitoring, verification and adjustment guidance from numerical weather prediction (NWP) models.

2. Types of image

Images from geostationary and polar-orbiting satellites are obtained using radiometers which measure the amount of electromagnetic radiation emitted and scattered by the Earth and its atmosphere. Radiation intensity is recorded over specific ranges of wavelengths. The main types of satellite images currently used operationally include visible (VIS) images, recorded in the range 0.4–0.7 micrometres; infrared (IR) images derived from radiation in the 10–12 micrometre waveband; water vapour images from the 6–7 micrometre band and images from 3.7 micrometre wavelengths, which is on the boundary between the VIS and IR regions.

A visible image, only obtainable on a daylight pass, measures the amount of sunlight reflected from the Earth's surface or from cloud tops. Infrared images effectively provide information on the temperature of the Earth's surface, or the cloud above it. These can be recorded at anytime during the day or night.

3. Interpreting satellite images

Distinctive patterns of clouds seen on satellite images help forecasters to recognize and track weather systems. For example, mature depressions are recognized by their distinctive swirl of cloud. Frontal systems often appear as wishbone-shaped areas of cloud radiating from a depression. The images can also be interpreted to provide information about the composition of the atmosphere and the vertical temperature profile. By measuring the changing position of clouds on successive images, it is possible to get an indication of wind speed at the cloud levels. Future developments will obtain and interpret satellite images to give an idea of surface wind strengths by studying the characteristics of ocean waves, and measure rainfall.

Geostationary satellites provide new images every half hour. These can be displayed as an animated sequence to show the movement and breakup of cloud systems, as well as to provide insight into the dynamic evolution of weather patterns and help in their early recognition.

4. Visible, infrared and water vapour images

In the visible radiation spectrum images are reflected sunlight from the Earth's surface or from the clouds above it. In general, the cloud thickness determines the brightness of the image.

Infrared images measure the infrared radiation emitting from surfaces. and provide an indication of the temperature of the Earth's surface or, where there is cloud cover, of the cloud tops. The images are often displayed on a grey scale with the colder surfaces appearing lighter, and the warmer ones darker. Infrared images make it possible to distinguish between high cloud, which appears white on the images because it is cold, and low cloud, which looks dark on the images because it is warmer.

Combined study of visible and infrared images can often resolve uncertainty. For example, if both images are bright in a particular area, the cloud is likely to be high and thick. However, if the visible image shows areas of bright cloud, but the same area in the infrared image is dark, this indicates that the cloud is low, or that there is fog present.

Radiation from moisture in the cold upper troposphere will appear white, in the water vapour image spectrum, and radiation from water vapour at warmer, lower levels in the troposphere will appear dark. Water vapour radiation from these lower levels will only be picked up if the colder upper troposphere is dry.

5. Geostationary satellites

Geostationary satellites, orbiting at a height of 36 000 km over the equator, travel at the same speed as the Earth rotates, and thus stay over a particular location on the Earth's surface. Five geostationary satellites, the European Meteosat, two US satellites (Goes-E and Goes-W), the Soviet GOMS satellite and the Japanese GMS satellite, together would provide complete coverage of the globe. Each geostationary satellite views a full earth-disc and is able to collect good quality data, with a resolution of around 4–5 km, up to latitudes of around 65 degrees north and south.

Each of the geostationary satellites is capable of making images of the Earth's surface, every half hour, although the images are usually made available hourly.

The data received from the geostationary satellites are usually presented the form of images which resemble black and white or false colour pictures of the Earth from space. The images can be interpreted to provide cloud, water vapour, and sea surface temperature maps. Because new images are available hourly, they provide a convenient way to monitor the movement and development of weather systems. Wind speeds can be estimated by tracking the movement of clouds.

6. Polar-orbiting satellites

Two US polar-orbiting satellites are currently providing coverage of the Earth. They orbit at an altitude of roughly 870 km, in a fixed position relative to the Sun, which means they always cross the equator at the same local time. The polar orbiters take about 1 hour 42 minutes to pass round the Earth. During this time the rotating Earth has moved on by about 25 degrees, so the satellite views a different part of the Earth's surface on successive passes. Each satellite passes over any given point on the ground every 12 hours, so with two satellites in orbit, pictures of any particular area are available every 6 hours.

Because the polar orbiters view the Earth from a lower height than do the geostationary satellites they are capable of providing much higher spacial-resolution data. They are also able to provide vertical profiles, or soundings, of temperature or humidity data in the atmosphere by measuring over a wide range of wavebands. This provides much useful data input for numerical weather forecasts. The satellite soundings also complement the very detailed local measurements made using radiosondes sent up from the surface by providing a global view.

7. International co-operation

Keeping meteorological satellites in space is an expensive business and relies very much on international co-operation. The United Kingdom is one of the 16 European nations contributing to the European Eumetsat organization, which is responsible for operating the Meteosat geostationary satellite. Currently, two of the polar-orbiting satellites are provided by the United States, also two by USAF and two by USSR, but much of the instrumentation on board is contributed by other countries, including the United Kingdom. However, by around 1997–98, Eumetsat expects to be taking responsibility for one of the polar satellites, and the involvement of the Meteorological Office will increase, with a corresponding rise in their budget for space activities towards 15% of the total budget.

International collaboration also extends to lending a satellite when the need arises. During the summer of 1991 when one of the US geostationary satellites reached the end of its life and its replacement was delayed due to technical difficulties, Eumetsat moved one of their satellites to a new position in order to fill the gap in coverage. Meteosat-4 will continue to stand in until the US replacement satellite is operational.

8. Not just for forecasters

Satellite images also have their uses outside the weather forecasting field. Recent work by zoologists at Oxford University has shown that data from meteorological satellites can be used to map the distribution of tsetse flies, a series disease carrier in humans and animals in some parts of Africa. Because the flies are restricted to the moister parts of the continent, the zoologists believe that satellite data provides an inexpensive and effective way of estimating the tsetse fly distribution over vast areas where rain-gauges are few and far between. This could provide an effective means of deciding where insecticides are most needed. A similar process is already used to combat the desert locust.

Other satellite images are used to map the distribution of disease-causing organisms. This has important implications for the health of developing nations.

9. Looking ahead

Meteorological organizations are continuously working on new developments to ensure that even better data is available from satellites in the future. They have to look ahead to keep ahead, because development time-scales tend to be in the order of decades.

In the short term, plans for improvement include replacing temperature measurements made in the infrared, which can only be collected in cloud-free areas, with microwave measurements, which are not affected by clouds. Looking further ahead, new techniques to improve vertical temperature resolution are being studied. These will lead to improvements in forecasts and will provide better data for numerical weather prediction models.

Some of the instruments of the future are already in use. The recently launched Earth Resources Satellite is carrying the first generation of active microwave instrumentation, in the form of a radar scatterometer which can give indications of features such as sea surface winds. Once their value for meteorology has been demonstrated, active microwave instruments may eventually form part of the standard instrumentation on weather satellites.

Although satellite data is expensive to obtain many would argue that as the only available source of global information, it is cheap at the price. Satellite data provides essential information for accurate very-short-term nowcasting and is one of the factors behind the dramatic improvement in numerical weather prediction models capable of providing forecasts for up to 5 days in advance. As the numerical models continue to improve, they will need even better data to get the best performance, and satellite data will become even more critical. Forecasters of the future will wonder how anyone ever lived without it.

10. Not forgetting radar

Radar provides a valuable source of information about rainfall, echoes being produced as the emitted signals are scattered from raindrops.

Areas of rain cause interference on radar screens, a nuisance for air traffic controllers, but meteorologists now use radar to detect areas of rainfall, and provide information on the intensity. The British Isles radar network consists of 12 radar stations and is part of a larger European network.

Rainfall maps can be constructed from radar information to display areas of no rain, and rates of rainfall of different intensity using different colours or shades of grey on a 5 km grid. The images are recorded at 15-minute intervals These are animated by displaying them in sequence to track showers and monitor their development. It is left to the forecaster to decide the type of precipitation.

(Information from Dr Peter Curtis, Mike Bader, Ken Wright and the book *Weather Facts* by Dick File.)

551.501.777:551.501.795:551.507.362.2(52)

The application of satellite infrared and passive microwave rainfall estimation techniques to Japan: Results from the First GPCP Algorithm Intercomparison Project

E.C. Barrett and T.J. Bellerby
Remote Sensing Unit, Department of Geography, University of Bristol

Summary

The contribution of the University of Bristol Remote Sensing Unit (RSU) to the Global Precipitation Climatology Project (GPCP) Algorithm Intercomparison Project (AIP) is discussed. This contribution comprised the production of monthly, daily and hourly rainfall estimates using GMS infrared and SSM/I passive microwave data. A number of variations upon, and extensions to, the Bristol PERMIT infrared technique were implemented. Rainfall estimates were also produced from passive microwave data alone using a combined 37 GHz Polarization Corrected Temperature (PCT)/19 GHz Polarization Difference technique. The results of the algorithms described are evaluated against a composite radar/rain-gauge product. A second AIP is being organized by the GPCP and the UK Meteorological Office to cover parts of north-west Europe during 1991/92.

1. Introduction

Under the direction of Dr P. Arkin, the World Climate Research Programme's (WCRP) Global Precipitation Climatology Project (GPCP) has been organized to produce a 10-year archive of estimated monthly precipitation for all 2.5° latitude/longitude areas between 40° N and 40° S from 1986 to 1995. Statistics of IR imagery from the GOES, Meteosat, Insat and GMS geostationary satellites, and NOAA polar-orbiting satellites are being collected and used to compute estimates of accumulated rainfall.

At the 3rd Session of the GPCP International Working Group on Data Management (IWGDM) held at Darmstadt, Germany, in July 1988 it was agreed that a pilot project for GPCP algorithm validation and development should be organized as soon as possible. An Expert Meeting was held in Washington DC in April 1989 to lay detailed plans for the project for which a special data set would be prepared and in which it was hoped that several laboratories from different countries would participate. This meeting agreed that the general objectives for the Japanese GPCP project should be as follows:

(a) To assess the skills of existing algorithms in extracting rain information from satellite imagery.
(b) To help understand why different algorithms yield different results.
(c) To improve existing algorithms.
(d) To ensure that the GPCP algorithm performs adequately for needs of the WCRP.

The University of Bristol Remote Sensing Unit (RSU) participated in the resulting GPCP Japan Algorithm Intercomparison Project by producing outputs to the agreed project specification from satellite rainfall algorithms already implemented and tested for other areas of the world. A considerable measure of further

algorithm calibration and development was necessary in order to apply the Bristol methods to the particular meteorological conditions prevalent in the study area over the study period. Throughout the course of the project it was the intention of the Bristol RSU to test several algorithms in sequence and generate a series of results which would elucidate the extents of the contributions made to rainfall estimates by different sources of satellite and collateral data.

The satellite methods to be used by the RSU were based on the objective Polar-Orbiter Effective Rainfall Monitoring Integrative Technique (PERMIT) infrared approach orginally developed for use with either NOAA or selected Meteosat imagery over Africa, and selected passive microwave methods already in the process of development at the RSU in conjunction with NASA, NOAA/NESDIS and the Meteorological Office.

1.1 The Intercomparison data set

The data for the First Algorithm Intercomparison Project were provided by the Japanese Meteorological Association in two parts. The first, containing satellite and meteorological model data for the study period, together with 9 years of precipitation climatology from ground stations, was to be used for the generation of rainfall estimates. The second, comprising rain-gauge and composite radar/rain-gauge data spanning the study period, was intended for verification purposes. Each data set spanned two month-long study periods: June 1989 (dominated by a persistent frontal regime, the 'Baiu') and 15 July–15 August 1989 (dominated by a tropical convective regime). The study area, and the included but much smaller region spanned by the validation data are shown in Fig. 1.

The following components of the initial data set were employed in this study:

(a) Hourly infrared GMS data for the study period. These images were stored on a latitude/longitude grid to a resolution of $0.05° \times 0.625°$.

(b) Passive microwave data. Data from the Special Sensor Microwave Imager on the Defense Meteorological Satellite Program (DMSP) Block 5D-2 Spacecraft were supplied for the study period. Data from this satellite should comprise dual-polarization measurements at 19.35, 37.0 and 85.5 GHz, plus vertical polarization observations at 22.235 GHz. In practice, the data for the intercomparison study were collected after partial failure of the 85.5 GHz vertical polarization sensor due to overheating. Data for the horizontal polarization at this frequency were available, but considered highly unreliable.

(c) Data from the Japanese Meteorological Association (JMA) Global Spectral Model. This comprised 12-hourly precipitation totals (to 0.01 mm) on a 1.25° grid together with daily values for sea level pressure, wind components, temperatures, heights and dew-points for standard atmospheric levels.

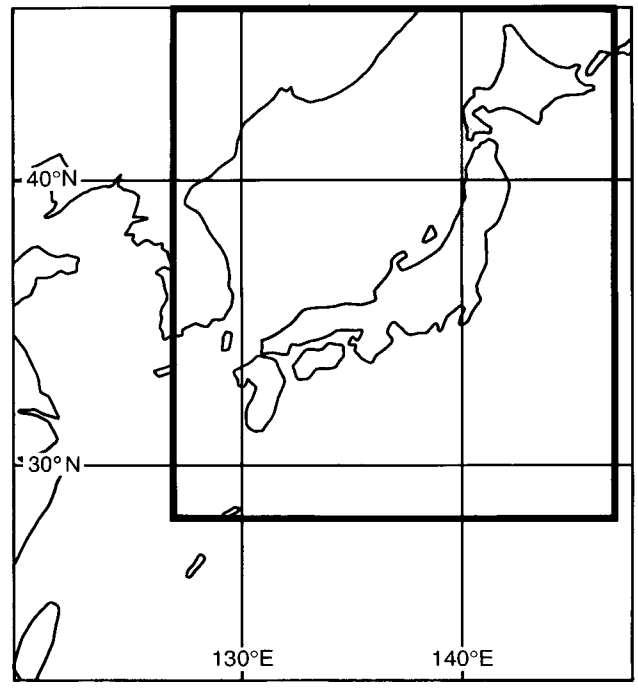

Figure 1. The area covered by the GPCP AIP dataset. The smaller area enclosing the composite radar/rain-gauge validation data set is also shown.

The validation data set, only supplied after the products derived from the initial data set had been supplied by participating laboratories including the RSU to the Algorithm Intercomparison Centre, comprised the following:

(a) Hourly Automated Meteorological Data Acquisition System (AMeDAS) radar/rain-gauge composite data to a resolution of 0.0625° longitude by 0.05° latitude covering a region bounded by 127°E and 147°E, 28°N and 46°N. The data comprised rain rates to a resolution of 1 mm h^{-1}.

(b) AMeDAS ground-station data comprising hourly and daily precipitation (mm), wind speed and direction, sunshine duration and temperature.

1.2 Intercomparison Project required products

The intercomparison study was based around the comparison of rainfall products produced by various participating groups using the first supplied data set only; as explained above, validation data was only supplied after the completed products had been submitted. The products required by the Algorithm Intercomparison Center (AIC) of the National Oceanographic and Atmospheric Administration (NOAA) consisted of the following:

For infrared algorithms:

(a) Fields of accumulated rainfall, to 0.1 mm, on a 1.25° grid covering the Japan study area, for each day during the two study periods.

(b) Time-series of accumulated rainfall for five specific areas, at the highest temporal resolution possible (up to hourly). The specified areas comprised

four 1.25° × 1.25° latitude/longitude boxes and a further 2.5° latitude/longitude box.

For passive microwave algorithms:

(c) Fields of rain rates, to 0.01 mm h^{-1}, at the highest spatial resolution available for ten specified swaths.

For all algorithms:

(d) Fields of accumulated rainfall, to 0.1 mm, on a 1.25° grid for the two monthly periods.

2. Methods and techniques employed

2.1 Infrared methods

The infrared products produced for the algorithm intercomparison were based upon variations of the Bristol PERMIT method (Barrett and D'Souza 1985, Barrett *et al.* 1986a, 1986b). Originally developed for a relatively long-period, convective regime, use with polar-orbiting satellite data, this technique seeks to identify rainy days rather than individual rain events. In the basic implementation, one or more occurrences of cloud colder than a fixed threshold are deemed sufficient to indicate that a pixel area has experienced some precipitation during a 24-hour period. Precipitation days so identified are assigned a rainfall equal to a mean-rain-per-rain-day statistic ('morphoclimatic weight'), obtained from climatological atlases or other sources. In previous work four images a day had been successfully employed to produce rainfall estimates for periods of 10 days or longer. However, given the availability of hourly GMS data in the Japan data set, the potential existed to produce effective estimates for considerably shorter time intervals.

The procedure described above generates first-order estimates based upon climatological predictors only. If synoptic data are available from local ground-stations, further corrections for meteorology become possible. In previous work, a piece-wise global linear correction function had been derived from a comparison of monthly rainfall estimates for ground-station locations and the rain-gauge data themselves. This function related the first order products generated by the initial stage of the algorithm to improved rainfall values more in accord with the meteorological data (Barrett and Richards 1989).

2.2 Modifications to the PERMIT algorithm for use over Japan

A number of significant differences existed between the intercomparison data set for the Japan study and the data sets used for previous applications of PERMIT. These included: the present availability of hourly infrared images for the study area, the lack of any calibration data for the first stage of the present study, and the availability of numerical model outputs and passive microwave data as possible additional inputs to the rainfall estimation process.

The choice of a temperature threshold for the identification of 'probably precipitating cloud' is a difficult procedure; no clear rules are available to determine the most appropriate values to use for different latitudes, climatic conditions, etc. In previous implementations of the PERMIT method the selection of the threshold temperature had been accomplished using a combination of information from atmospheric soundings and the experience of implementors. Given the complexity of the weather regimes around the Japan test area, involving both tropical and mid-latitude systems, significant advantages were seen in the employment of a more objective approach to the choice of the key cold-cloud threshold. The initial stage of the PERMIT method is primarily a mechanism for identifying rainy days. This property of the algorithm implies that the utility of any particular threshold function must be assessed by the precision to which its application generates rain-day counts. To this end, optimal thresholds were obtained by matching, in a broad statistical sense, rain-day-count outputs from the front end of the PERMIT algorithm with equivalent precipitation-day information derived from collateral data for the study area.

Two sources of collateral rain-day data were employed for the generation of suitable cold-cloud thresholds, namely climatological data from Takahasi and Arakawa (1981) and outputs from the JMA Global Spectral Model. The former were only available for a limited number of randomly distributed ground-station locations while the latter were available for all points on a 2.5° grid covering the study region (and areas beyond). Although it would be possible to define a threshold function which varied with both spatial dimensions, the sparseness of the collateral data suggested that for present purposes it would be more practicable to derive cold-cloud thresholds which varied with latitude alone.

The study region was split into a number of regions, each of which spanned a 2.5° range in latitude. Area-averaged rain-day outputs for each region were produced using a range of fixed cold-cloud thresholds. Equivalent regional statistics derived from the collateral data sources were then matched to these products, yielding an optimal threshold value for each latitude range. Cubic spline interpolation produced cold-cloud thresholds which were a smooth function of latitude (Fig. 2). The use of climatological data for threshold selection proved unsatisfactory over the July–August period — a combination of the available monthly statistics for July plus August did not produce reliable rain-day counts for the intermediate period from 15 July to 15 August and these counts in turn gave rise to totally unconvincing threshold functions. Hence PERMIT runs for this later study period exclusively employed the thresholding functions derived from JMA model data.

The same two sources of collateral data (climatological records and numerical model outputs) used to generate cold-cloud thresholds were employed to derive the required background fields of morphoclimatic weights. For the climatological source, mean-rain-per-

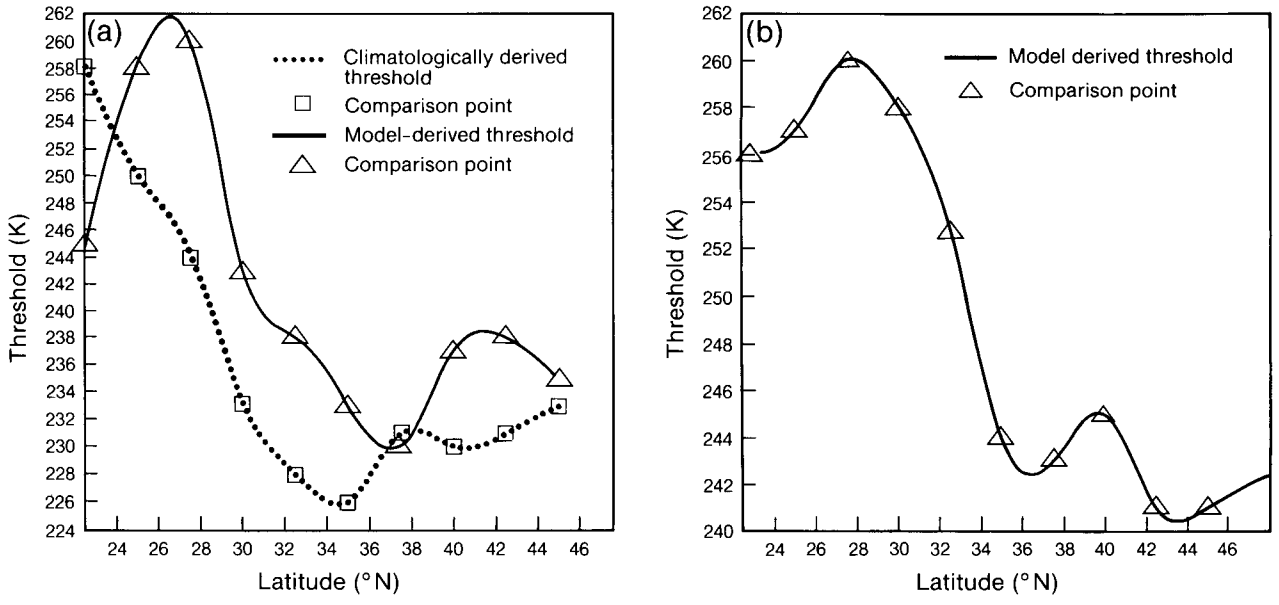

Figure 2. Cold-cloud thresholds for the PERMIT algorithm for (a) June 1989 and (b) 15 July–15 August 1989.

rain-day values for the various climatological stations were plotted on a map onto which, taking account of the local geography, the contours of the overall morpho-climatic weight field were drawn by interpolation. The resulting contour map was digitized and interpolated to the required 441 × 476 grid using a simple algorithm employing repeated 3 × 3 selective mean filtering (Fig. 3(c)). The model-derived background field of morphoclimatic weights was interpolated from the 2.5° square grid of the JMA Global Spectral Model precipitation product using the same successive filtering technique (Figs 3(a) and 3(b)).

When combining the various possible permutations of the two sources for each of the two non-satellite inputs to the algorithm, it was discovered that the most reasonable results came from matching the data sources used to derive both the thresholds and the morpho-climatic weights. Errors of a relatively small magnitude in the model precipitation estimates had a significant effect upon the number of rain-days counted by the thresholding of daily rainfall totals above 0.25 mm. When the model-derived rain-day products were used to generate both functions and background weights, the errors introduced by these inaccuracies tended to cancel themselves out; in contrast, mixing input sources lead to a considerable over- or under-estimation of total rainfall.

When the validation data set was received it was found that this contained rainfall totals to a resolution of only 1 mm. It was therefore not possible to use this data set to assess directly the procedures used to derive threshold functions and background fields of morpho-climatic weights. Such an investigation would have required data with at least 0.25 mm resolution if rain-day counts could be derived and compared.

2.3 Extending the PERMIT algorithm to produce daily rainfall totals and time-series to a resolution of one hour

The basic PERMIT technique is a good estimator of long-term rainfall totals but gives little information on the distribution of individual precipitation events. This property of the algorithm is a deliberate result of its structure; precipitation events are assigned rainfall values in such a manner as to ensure correct long-term totals rather than accurate instantaneous rain-rate estimates. In order to generate rainfall products for shorter periods without sacrificing this basic advantage of the algorithm, the PERMIT technique was modified in such a manner as to leave unchanged any longer-term, larger-scale rainfall totals, but to ensure that daily and even hourly estimates might be as accurate as possible.

Fig. 4(a) shows a simple, linear function relating the effective number of rain-days represented by one rainy day (daily rainfall divided by mean-rain-per-rain-day) to the cold-cloud count for that day. This function was derived by noting that the mean number of mean-rain-days rainfall for sufficiently large data set must, by definition, be equal to the mean number of rainy days. Using this constraint, the slope of the linear function could be calculated simply from the occurrence histogram for the 24 possible daily cold-cloud events taken over the entire infrared data set (Fig. 4(b)). From Fig. 4 it may additionally be seen that the true slot-weight function (mean radar/rain-gauge derived rainfall associated with each slot-count category) is non-linear. However, the low frequencies at which the higher slot counts occur (Fig. 4(b)) do permit some deviation from linearity without significant alteration to the magnitudes of any resulting rainfall estimates. It should be noted that this method of assigning daily rainfall leaves the

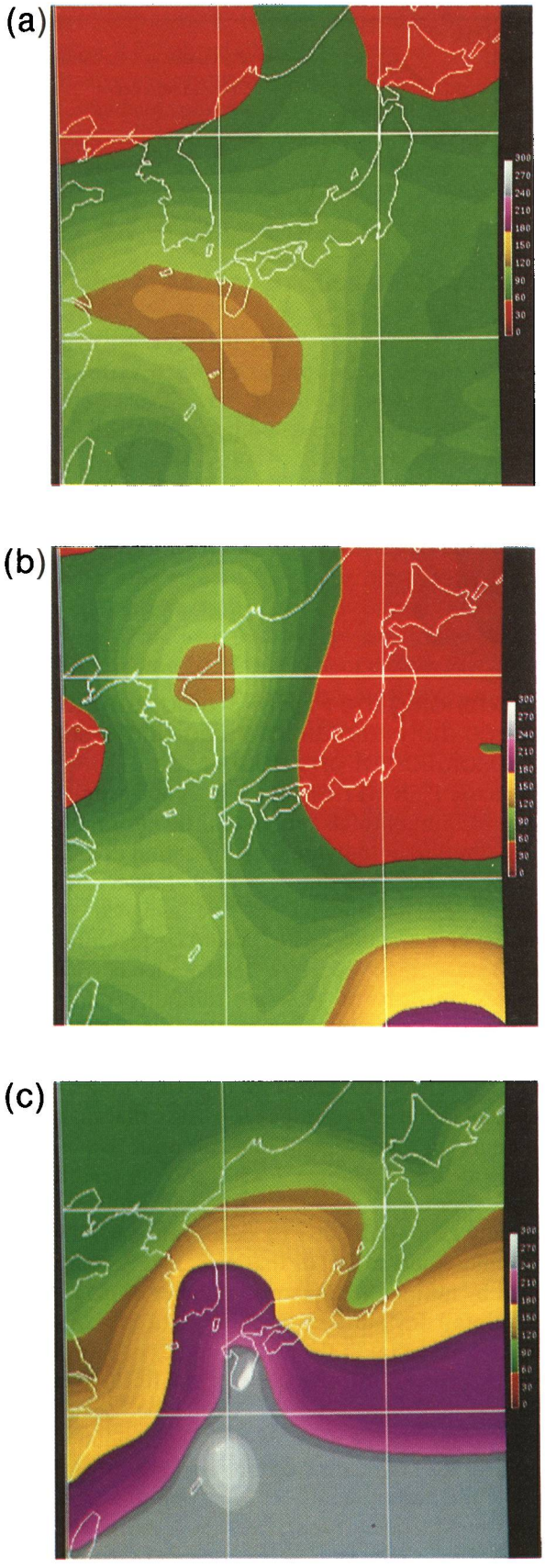

Figure 3. Backgrounds fields of morphoclimatic weights. The values on the scale indicate tenths of millimetres rainfall for (a) June 1989 derived using JMA model data, (b) 15 July–15 August 1989 derived using JMA model data, and (c) June 1989 derived using climatological data.

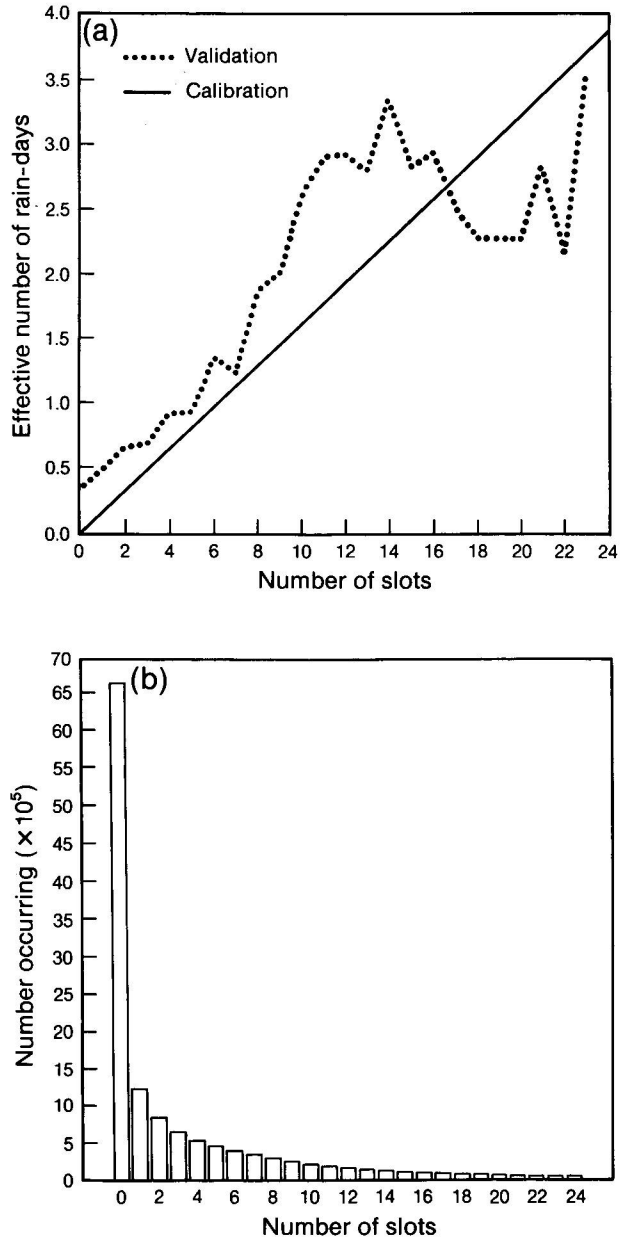

Figure 4. (a) The linear function used in the PERMIT algorithm to relate daily rainfall (in terms of the mean-rain-per-rain-day) to the cold-cloud count for that day. Also shown is the 'true' function relating mean daily rainfall (in terms of the mean-rain-per-rain-day) to the cold-cloud count for that day, derived by comparing the PERMIT products to the composite radar/rain-gauge validation data, and (b) frequency histogram for daily cold-cloud counts derived from the entire AIP infrared data set using model-output derived temperature thresholds.

mean number of mean rain-days rainfall for the entire study area over the entire study period unchanged with respect to the output from the basic PERMIT algorithm; the daily estimates may be said to be derived by a form of 'weighted interpolation' from the longer-term product. Continuing this same 'progressive-refinement' approach, hourly rainfall estimates were obtained by equally dividing each daily rainfall estimate between the identified cold-cloud events for that day.

2.4 Correction of PERMIT outputs using rain-gauge data

While the initial data set for the intercomparison study did not contain any ground data, the validation data set included both rain-gauge data and a combined radar/rain-gauge product. The former of these two data sets was used to derive a correction function for selected infrared products, the corrected versions of which could then be verified against the latter, composite, product. Previous work involving the improvement of PERMIT products using data from ground-stations had concentrated upon the derivation of a global non-linear correction function relating preliminary rainfall estimates to improved values more closely reflecting the ground data. In the case of the Japan study data, however, the primary discrepancy between the rainfall products and the validation data involved a lack of detail in the former with respect to the structure of the rainfall distribution over the islands of Japan. For this reason a simple multiplicative correction factor was calculated for each ground-station based upon the ratio of estimated to observed monthly rainfall and interpolated using a repeated 3×3 selective averaging filter to derive a global, spatially varying, field of correction factors.

2.5 Passive microwave techniques

A considerable amount of research concerning the extraction of rain area and rain-rate information from passive microwave products had been conducted at the RSU prior to the commencement of the Japan Algorithm Intercomparison Project (e.g. Kidd 1988, Kidd and Barrett 1990). However, a number of severe deficiencies in the passive microwave data supplied with the intercomparison data set significantly hindered the generation of both instantaneous and accumulated rainfall products by the methods which had been developed at Bristol for these purposes. The most severe difficulty encountered was the lack of data from the 85 GHz vertical channel, compounded by serious doubts about the quality of the 85 GHz horizontal channel data. This problem precluded the implementation of the RSU Bristol's preferred rainfall-estimation technique for mixed land/sea areas — a polarization-corrected temperature (PCT) algorithm operating at 85 GHz, calibrated against a 85 GHz/37 GHz frequency difference algorithm operating over land areas only. An additional difficulty resulted from the lack of any proper calibration data set for the Japan Project as a whole. This substantially hindered the assessment and calibration of any replacement technique.

The algorithm eventually chosen comprised:

(a) Over sea areas uncontaminated by proximity to land, a polarization difference technique operating at 19 GHz using a global calibration already developed at the RSU Bristol for other purposes (Barrett and Kidd 1991)

(b) Over land and coastal areas, a 37 GHz polarization-corrected temperature technique (Grody 1984), separately calibrated for each monthly period against the polarization difference method by comparing respective values for points within sea areas uncontaminated by land.

Preliminary investigations into the use of the passive microwave data over Japan employed a slightly different algorithm, identical to the above except that a 37 GHz polarization difference technique was used over the sea. This provisional method, which employed an earlier, less effective, global calibration, considerably overestimated all rainfall totals. Parallel research in progress at the RSU yielded improved calibrations for the polarization difference technique at both 19 GHz and 37 GHz and additionally indicated that the lower frequency channel gave a better response for higher rainfall rates. These two factors lead to the adoption of the final algorithm described above.

To summarize:

$$\text{Rainfall} = f(V_{19} - H_{19}) \text{ (over open sea)}$$

$$= g\{(1+\Gamma)V_{37} - \Gamma H_{37}\} \text{ (over land or coastal areas)}$$

Here f and g are piece-wise linear functions, V_{37} is the vertical brightness temperature at 37 GHz and H_{37} is the horizontal brightness temperature at the same frequency. Fig. 5 shows the mask used to classify land, sea and coastal areas.

The Γ parameter to the PCT algorithm was separately calculated for each of the monthly study periods through a comparison between the 37 GHz vertical channel brightness and polarization difference values occurring over uncontaminated land areas and the same variables measured over uncontaminated sea areas. Polarization differences and PCT values could then be compared over the ocean to calibrate the latter method in terms of rain-rates. All calibrations comprised piecewise linear functions. Pixel-resolution 'monthly' rainfall totals were obtained by compiling mean rain-rate statistics in mm h^{-1} for each pixel and multiplying these average values by the total number of hours in the appropriate 30- or 32-day period. The required grid of 1.25°-resolution monthly rainfall values were derived using a weighted averaging technique which took account of the number of individual overpasses contributing to each monthly accumulated pixel value.

Fig. 6 shows the PCT calibration functions for each month together with equivalent curves derived from the validation data (mean PCT) associated with each rain-rate category. The calibration functions are several degrees too severe, indicating that the algorithm should, as a whole, underestimate the amount of rainfall.

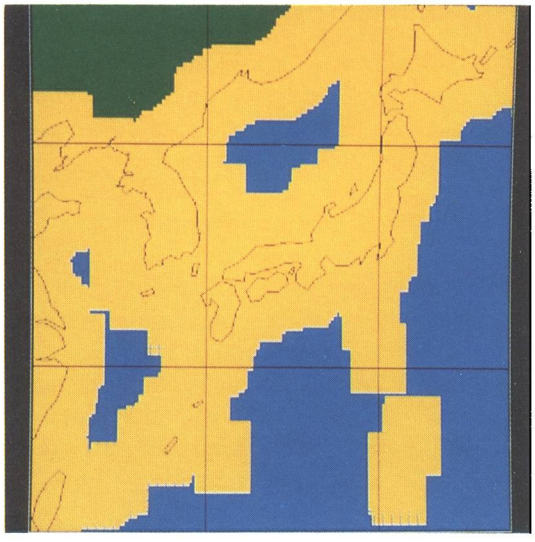

Figure 5. The mask employed to classify land, sea and mixed land/sea (coastal) areas in the passive microwave algorithms.

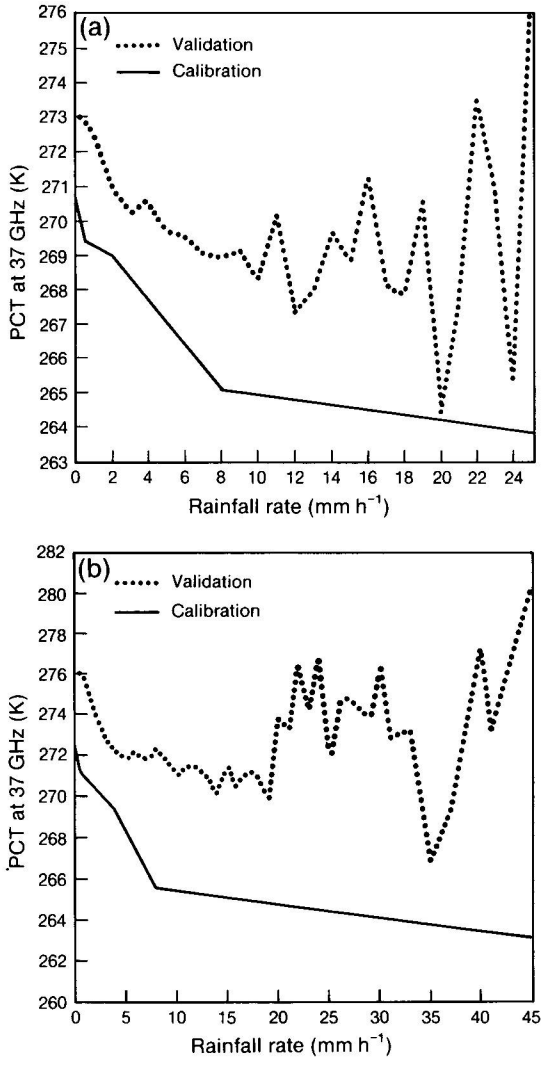

Figure 6. The PCT calibration functions used in the second passive microwave technique together with the 'true' calibration functions (mean PCT associated with each rain-rate category) derived by comparing the passive microwave and composite radar/rain-gauge data set for (a) June 1989, and (b) 15 July–15 August 1989.

3. Results

The primary purpose of the RSU study was to provide intercomparison products for the GPCP project which could then be compared with results produced by other centres using alternative algorithms, ultimately providing valuable information upon the relative strengths and weaknesses of different satellite rainfall monitoring strategies. This central comparison is currently being performed by the Algorithm Intercomparison Centre of NOAA, and the results are scheduled to be available later in 1991. Much of the work performed by the RSU with regards to the First GPCP Algorithm Project was algorithm development; this has been discussed in the section on development of methods and techniques (section 2).

Upon receipt of the validation data set it was possible to perform a preliminary evaluation of the effectiveness of the various algorithms developed throughout the course of the Japan Study. These results are presented here. Fig. 7 shows the monthly rainfall for June 1989 and for July–August 1989 derived from the composite rainfall/rain-gauge product supplied as a part of the validation data set. The most notable feature in these products is the diminution of rainfall with distance from the Japanese mainland; a number of zero monthly rainfall totals (highlighted in white) ring the validation area. This fall-off suggests that radar range effects have a strong influence upon the composite product. While there will certainly be some concentration of rainfall over the mainland, such a relationship will be difficult to differentiate from the radar range effects. As a consequence of this problem we believe that the algorithm validation exercise may take the form more of an intercomparison, between satellite techniques and the radar/rain-gauge composite method, than of a direct comparison/validation of the former.

Figs 8–11 show the estimated total monthly rainfall distributions for the two study periods (June 1989 and July 15–August 15 1989) while Table I gives r.m.s. errors between the various 1.25°-resolution monthly rainfall products and the validation data. The best results were produced by the model-calibrated version of the PERMIT infrared algorithm; the better of the two pure passive microwave algorithms generated estimates with twice the error magnitude of this infrared technique. In general, the infrared based results for the July–August period were much less satisfactory than those for June. There are a number of possible reasons for this: for example the PERMIT method may be less suited to the tropical convective regime predominating during the later period than to the persistent frontal regime ('Baiu') present in June; the July–August period may be untypical, deviating considerably from climatological norms and numerical model predictions; or the validation data for the latter period may be less representative than those for June, creating a false impression that one set of infrared derived results are more satisfactory than the other.

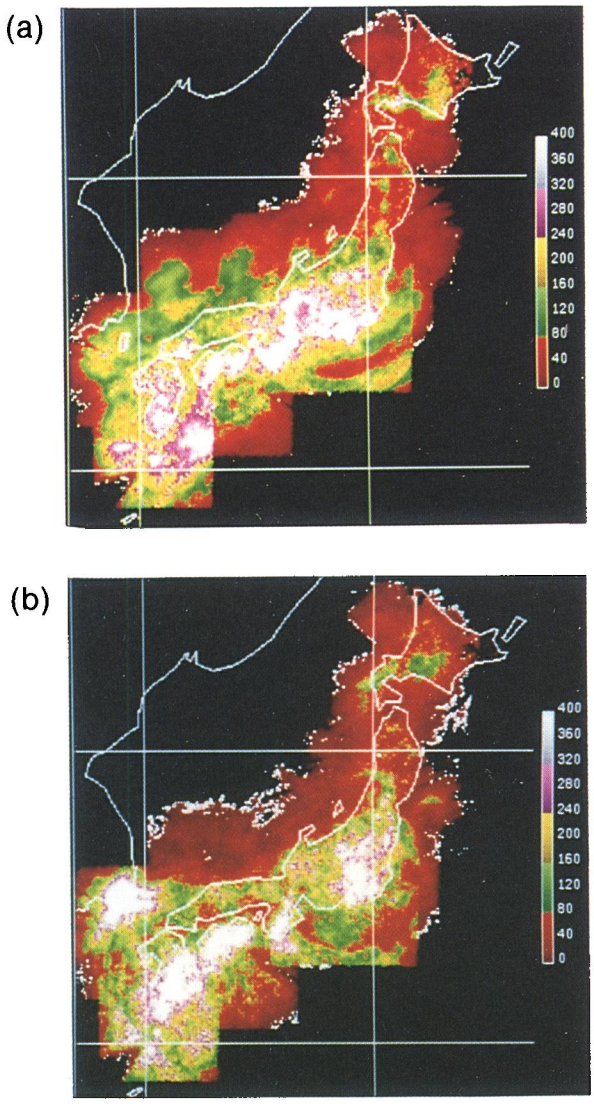

Figure 7. Monthly rainfall derived from the composite radar/rain-gauge product supplied as a part of the AIP validation data set for (a) June 1989 and (b) 15 July–15 August 1989.

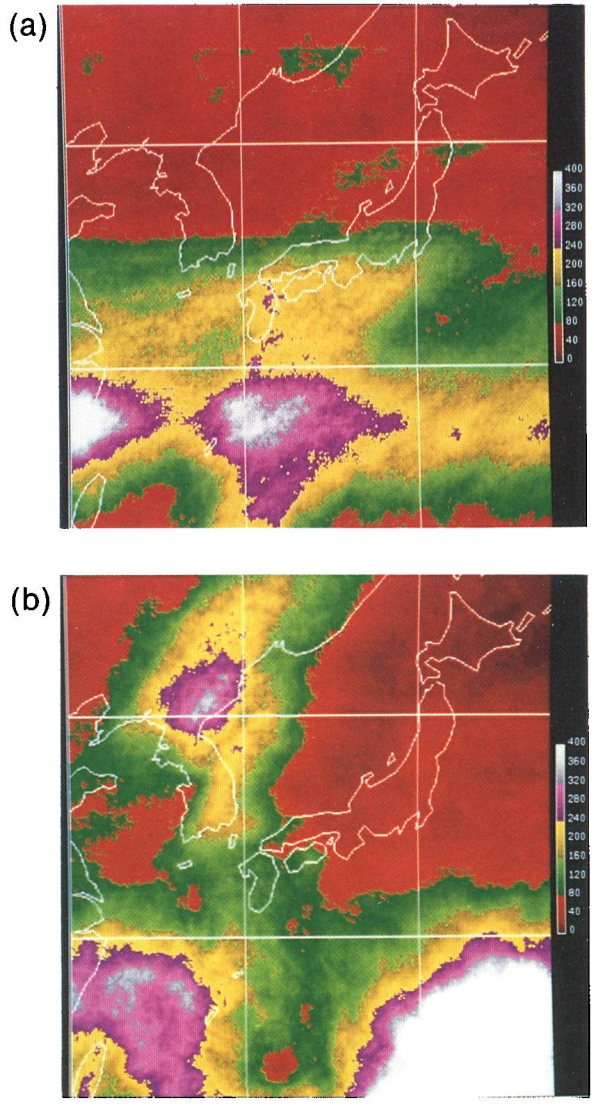

Figure 8. Model-calibrated PERMIT monthly products. The scale indicates monthly rainfall totals (mm) for (a) June 1989, and (b) 15 July–15 August 1989.

Table I. R.m.s. differences between monthly rainfall 1.25°-resolution products and validation data

Product	R.m.s. error (% of mean rainfall) June 1989 (mm)	(%)	15 July–15 August 1989 (mm)	(%)
Model-calibrated infrared	72.5	(47)	122.0	(81)
Climatologically calibrated infrared	100.4	(66)	N/A	
SSM/I	148.7	(97)	187.0	(113)
SSM/I infrared	123.0	(81)	105.7	(71)

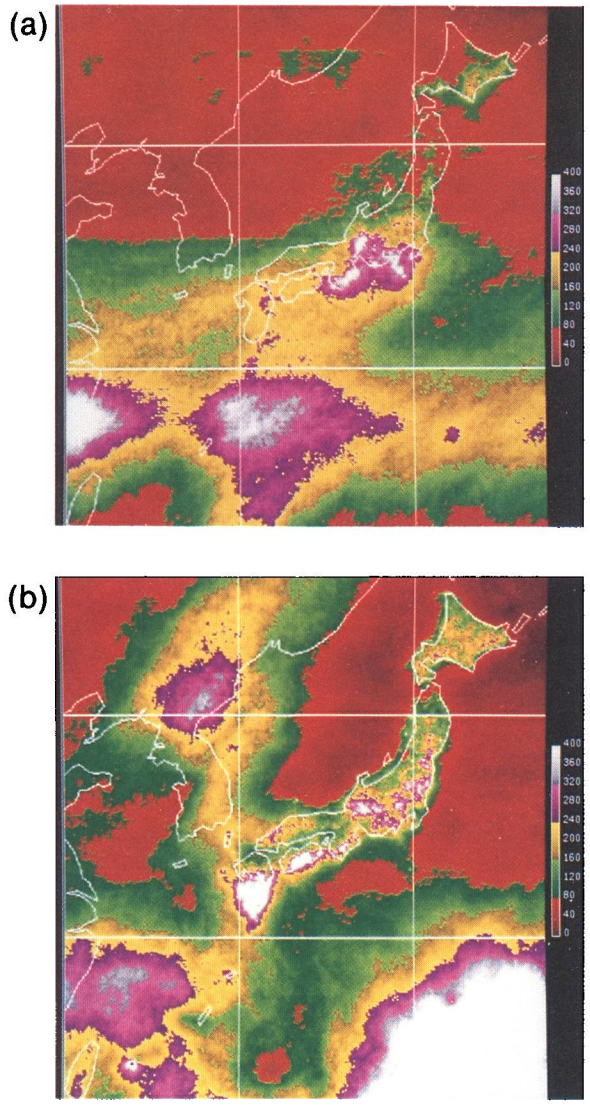

Figure 9. Model-calibrated PERMIT monthly products corrected using ground data. The scale indicates monthly rainfall totals (mm) for (a) June 1989, and (b) 15 July–15 August 1989.

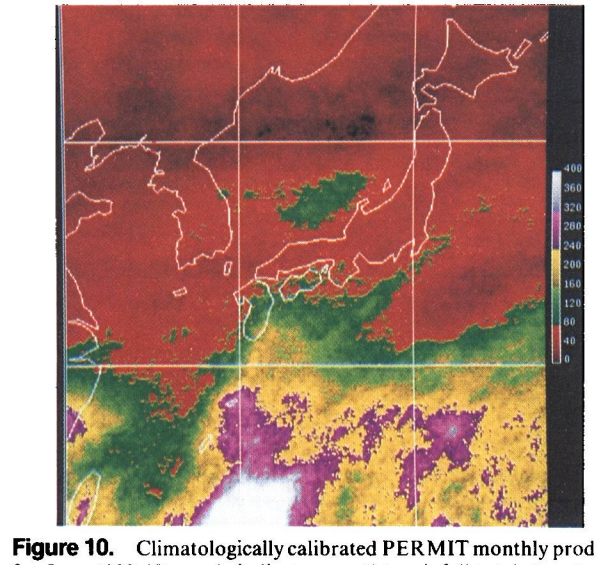

Figure 10. Climatologically calibrated PERMIT monthly products for June 1989. The scale indicates monthly rainfall totals (mm).

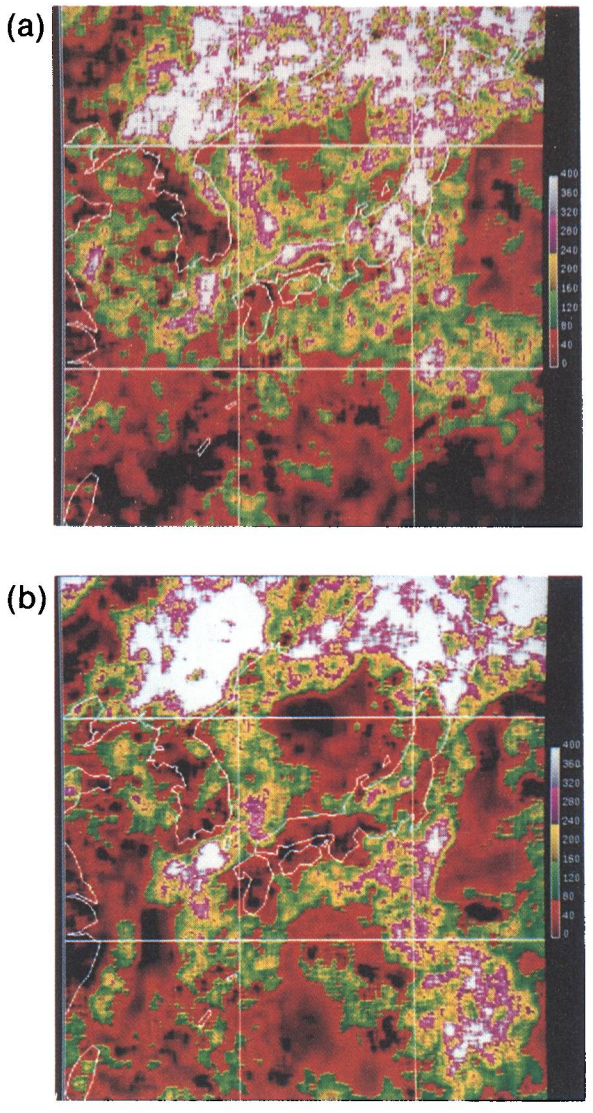

Figure 11. Monthly products produced using the passive microwave algorithm. The scale indicates monthly rainfall totals (mm) for (a) June 1989, and (b) 15 July–15 August 1989.

The poor quality of the passive microwave results with respect to calibrated infrared outputs may be attributed to a number of causes, chief among which may be as follows:

(a) The bulk of the passive microwave estimates for the validation area were produced using the 37 GHz PCT algorithm. Previous work at the Bristol RSU on PCT algorithms had concentrated upon the 85 GHz channels; the method has not adapted well to the lower frequencies available for this project.
(b) The return rate of SSM/I overpasses was poor. Fig. 12 maps the number of overpasses visiting each part of the survey area over June 1989. While it is reasonable to estimate monthly rainfall from just under two overpasses per day, the lower sampling rates encountered in the Intercomparison Data Set

Figure 12. The number of SSM/I overpasses for each pixel for June 1989.

will give rise to significant sampling errors (Laughlin 1981).

(c) The 85 GHz PCT algorithm has been found to perform less well than simple frequency or polarization difference algorithms over open land and open sea areas respectively. The nature of the study region, however, was such that the bulk of the pixel areas had to be classified as 'coastal', i.e. mixed sea or land, or close enough to land or sea to suffer from contamination of the reading and/or errors in swath position.

(d) A variety of meteorological regimes existed within the study area, which itself spanned more than 20° of latitude. Previous work at the RSU had shown that the 'gamma' parameter of the PCT algorithm should be varied with latitude and meteorological regime. The calculation of this parameter for any particular region, however, requires the presence of uncontaminated sea and land areas. The geography of the test area allowed only one, global, value for gamma to calculated.

The combined passive/microwave infrared technique appears to give a better result than the passive microwave data used alone. Given an effectively calibrated passive microwave algorithm operating upon a more complete data set, this technique could show considerable potential, combining as it does the rainfall-resolving properties of the SSM/I instrument with the high spatial and temporal resolutions of the infrared data to provide an effective, purely satellite-based, product.

Table II shows the contributions made by the various components making up the monthly corrected model-calibrated infrared product. The first entry shows the results of employing the calibration data alone. This product was produced by interpolating between rain-day counts derived from the collateral data for each 2.5° latitude range rather than the temperature threshold values derived from these counts. In this manner a field of rain-day counts was produced directly from the collateral data without employing the infrared imagery. Multiplication of this latitudinally varying field of rain-day values by the background field of morphoclimatic weights produced a rainfall product indicative of the contribution of the collateral data to the overall precipitation estimation process. The entries which follow the Table II show the errors for the unweighted and weighted PERMIT products and the weighted PERMIT product corrected using rain-gauge data. Figs 13–15 show this comparison in graphical form.

Table II. Comparison of monthly 1.25°-resolution rainfall products and validation data for various stages of the enhanced PERMIT algorithm

Inputs	R.m.s. error (% of mean rainfall) June 1989 (mm)	(%)	15 July–15 August 1989 (mm)	(%)
Calibration data	70.1	(45)	119.5	(80)
Calibration data + IR imagery	61.8	(40)	115.4	(77)
Calibration data + IR imagery + weighting function	72.5	(47)	122.0	(81)
Calibration data + IR imagery + weighting function + rain-gauge data	45.0	(29)	65.0	(43)

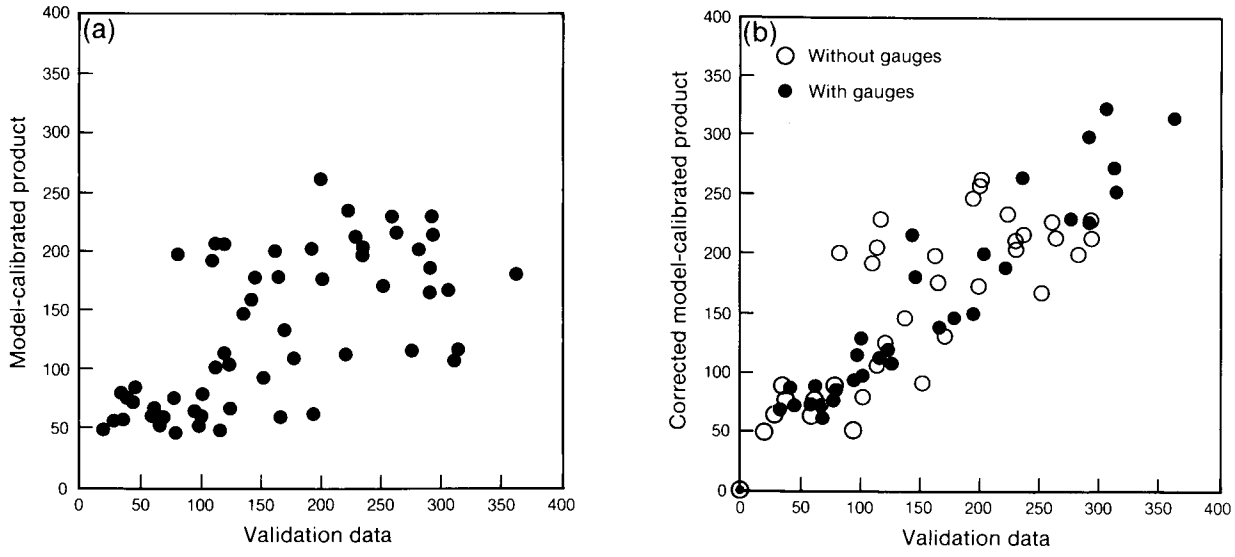

Figure 13. Scatter plots showing a comparison of monthly 1.25°-resolution model-output-calibrated PERMIT products for June 1989 and equivalent values derived from the composite radar/rain-gauge validation data set, (a) not corrected using ground data, and (b) corrected using ground data.

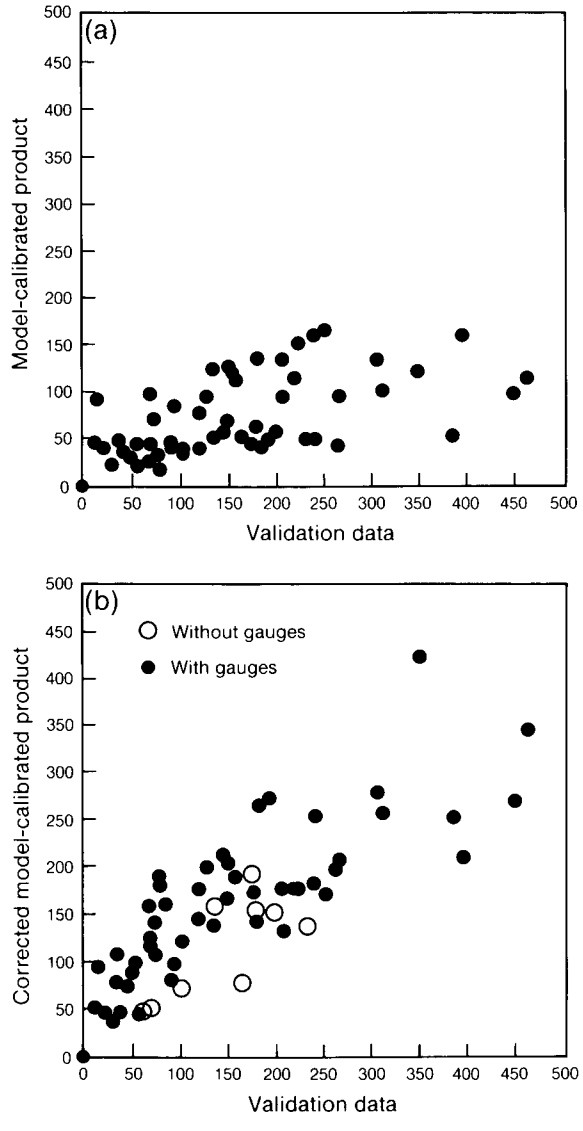

Figure 14. As Fig. 13 but for 15 July–15 August 1989.

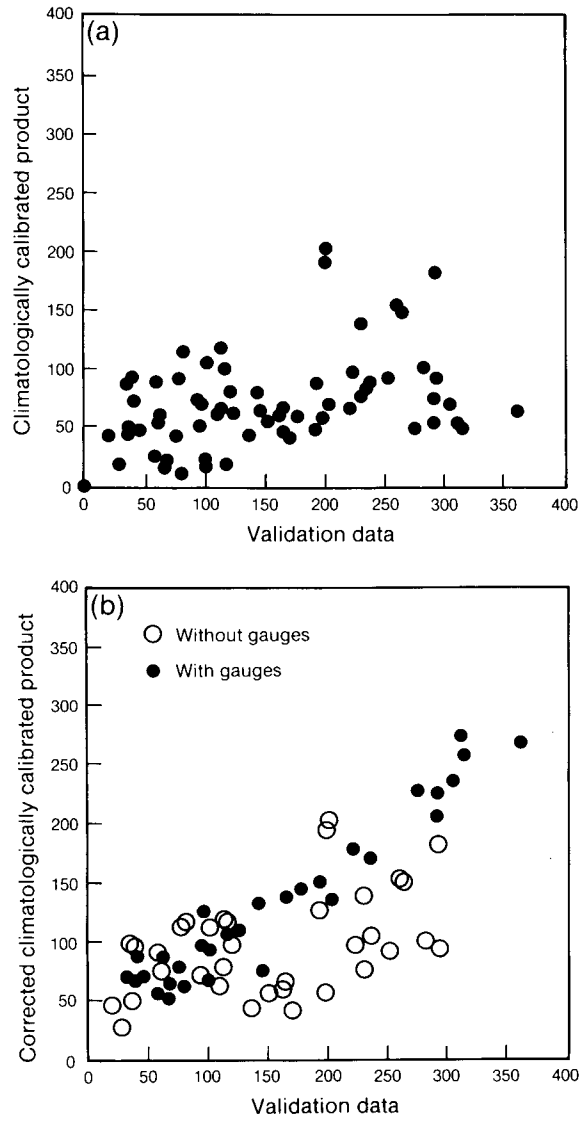

Figure 15. As Fig. 13 but for climatologically-calibrated PERMIT products.

Table III shows the errors in the daily estimates for the same series of products. In this case the collateral-data-only product was derived by evenly dividing the appropriate monthly product between the days of that month.

The inclusion of each data source (collateral, satellite, rain-gauge) creates a successive improvement in the rainfall estimates. The employment of the slot-count weighting function improved the daily estimates but degraded the monthly results to the point where the satellite input has no effect! This last result vindicates the use of the progressive refinement approach employed to improve the temporal resolution of the PERMIT method. Indeed, in light of these comparisons, it may be concluded that no attempt should have been made to improve the monthly estimates using slot-count information at all. A more strict implementation of the progressive refinement philosophy may well produce better daily estimates. For example, monthly estimated rainfall totals produced by the basic PERMIT algorithm could be unevenly distributed among the days of each month with the relative magnitude of each daily rainfall estimate related to the slot count for that 24-hour period.

4. Conclusions

Participating in the Pilot Algorithm Intercomparison Project of the GPCP, the RSU has successfully modified a number of satellite rainfall algorithms to operate over Japan. The PERMIT infrared algorithm was greatly enhanced to meet the product requirements of the intercomparison study. A number of promising new approaches to satellite rainfall monitoring techniques have been investigated. In particular, the progressive refinement approach used to enhance the PERMIT method appears to provide an effective strategy for the optimal extraction of rainfall information from infrared imagery despite the rather poor correlation of cloud-top temperature to rainfall area, intensity and duration. Also a combined passive microwave/infrared technique has been developed which gave an improved result over pure passive microwave techniques for the Japan data set.

These conclusions represent only a part of the scientific yield of the project. The comparison of the RSU products with results from other groups may be expected to generate considerable information upon the strengths and weaknesses of different satellite rainfall estimation strategies.

The GPCP AIP is part of an ongoing programme: a further algorithm intercomparison study, taking into account the lessons learned in the pilot Japanese study, is now being planned. This new study will cover a region of north-west Europe for a period in the late winter and early spring of 1991.

The use of the new progressive refinement approach to the generation of rainfall products from satellite and collateral data merits further investigation. In particular, much more work needs to be undertaken on the realistic assessment of the contribution made by each data source to the final product and upon the optimal integration of these individual components so as to maximize the information content of the final rainfall estimates. The results obtained from the validation stages of the present study indicates that the approach adopted did not employ the progressive refinement strategy to a sufficient extent, although to have done so would have been to be wise before the event. It would now be profitable to investigate a technique in which longer-term products are obtained from satellite images and other sources using one process, and then used in the derivation of shorter-term rainfall products by a completely separate procedure. In this manner the two stages could be independently developed and calibrated

Table III. Comparison of daily 1.25°-resolution rainfall products and validation data for various stages of the enhanced PERMIT algorithm

Inputs	R.m.s. error (% of mean rainfall) June 1989 (mm)	(%)	15 July–15 August 1989 (mm)	(%)
Calibration data	16.12	(187)	15.91	(215)
Calibration data + IR imagery	14.77	(171)	14.99	(203)
Calibration data + IR imagery + weighting function	13.73	(160)	13.22	(179)
Calibration data + IR imagery + weighting function + rain-gauge data	12.72	(148)	13.31	(180)

so as to make optimal use of all available data. Such an approach seems likely to be the best suited to presently available types of satellite and collateral data.

Further development of the combined passive microwave/infrared algorithm developed as a part this project would certainly benefit from the further application of the above strategy. The availability of a complete SSM/I data set including 85 GHz channel information would facilitate a much more realistic evaluation of this promising technique.

Acknowledgements

This Bristol participation in the GPCP AIP was funded by NERC under research grant GR3/7405.

References

Barrett, E.C. and D'Souza, G., 1985: The development of an objective range of dry day products for drought monitoring by Meteosat over Africa. Final Report for ESA and EARSeL (31 Dec. 1985) ESA Contract No. 6137/84/D/JS(SC).

Barrett, E.C., D'Souza, G. and Power, C.H., 1986a: Bristol techniques for the use of satellite data in raincloud and rainfall monitoring. *J Br Interplanet Soc*, **39**, 517–526.

Barrett, E.C. and Kidd, C., 1991: The mapping and monitoring of rainfall and other key variables by the SSM/I: some global and regional results. Final Report (Stage II) to the Universities Space Research Association, Columbia MD.

Barrett, E.C., Power, C.H., Beaumont, J., and Richards, T.S., 1986b: Cloud cover and rainfall in the Western Sahel. Final report to the NERC, Contract No. F60/C1/19 (30 June 1986).

Barrett, E.C. and Richards, T.S., 1989: Towards an operational system for the use of AVHRR data in Pakistan. Remote Sensing for Operational Applications. Technical Contents of the 15th Annual Conference of the Remote Sensing Society (13–15 September 1989), 41–46.

Grody, N.G., 1984: Precipitation monitoring over land from satellite using microwave radiometry. International Geoscience and Remote Sensing Symposium (IGARSS 1984). Strasbourg, France, 27–30 August, ESA SP-215-417-423.

Kidd, C., 1988: Passive microwave monitoring of rainfall over land. Ph.D. thesis, University of Bristol.

Kidd, C. and Barrett, E.C., 1990: The use of passive microwave imagery in rainfall monitoring. *Remote Sensing Rev*, **4**(2), 415–450.

Laughlin, C.R., 1981: On the effect of temporal sampling on the observation of mean rainfall. Precipitation measurements from space, Workshop Report. Goddard Spaceflight Centre, Greenbelt, MD. p D.59-D.66

Takahasi, K. and Arakawa, H., 1981: World survey of climatology. Vol. 9, Climates of Southern and Western Asia. Editor-in-Chief H.E. Landsberg. Amsterdam, Elsevier Scientific.

551.551:551.553.6(425)

Are gusts and lulls associated with directionality?

A.J. Baran

Meteorological Office, Bracknell

Summary

The question 'do gusts back or veer?' is addressed. It is generally believed that a gust should veer and a lull should back. This belief is tested using sonic anemometer wind measurements carried out by the Meteorological Research Unit at Cardington. The data represent near neutral and unstable conditions and were measured at a height of 6 m and 20 m on the 6 July 1990 and 19 June 1990 respectively. The resulting gusts and lulls have been analysed statistically by fitting a von Mises Probability Density Function to the gust and lull frequency distributions. From the data collected on the 6 July 1990 there is not enough evidence for asymmetry in the gust distribution to be able to state that gusts have a directional tendency. From the data collected on the 19 June 1990 there is evidence for an asymmetric gust frequency distribution but there is no evidence for asymmetry in the lull frequency distribution. A 10-second block average filter was applied to the 19 June 1990 data set in order to examine longer duration gusts. The results from this analysis indicate that there is no evidence, at the 5% level of significance, of asymmetry in the gust and lull frequency distributions. It is concluded that there is at most only very weak evidence for gusts and lulls being associated with a preferred direction.

1. Introduction

The motivation for the study of the veering of wind in gusts has come chiefly from the observed effects of gusts on structures, where the rapid fluctuations give rise to large lateral forces on a structure. This is particularly important from the point of view of wind turbines, as wind loading and wind directionality are important considerations for design. If gusts do have a directional tendency then this would be an important consideration at the design stage of a structure. Kristensen (1989) using different engineering examples, such as a building and an aeroplane, has constructed gust definitions for these situations.

It is generally believed that the wind veers in gusting. This is certainly believed by mariners and pilots: see for example Meteorological Office (1967, 1971). These books state, as literal truth, that the wind veers in gusts, but is the statement correct? The belief comes about because it is generally thought that a gust must be due to

winds that originate higher in the atmosphere and, since winds veer across the boundary layer, low-level gusts must also veer. However, there are problems associated with this belief. Gusts are a turbulence phenomenon and turbulence can arise from frictional surface effects, shearing and convection. The frictional surface effect is determined by surface properties and should have no systematic influence on wind direction. If shear turbulence is produced locally then the gusts would not represent faster moving air being brought down from a higher level in the atmosphere to the surface, so there would be no reason for the winds to veer in gusts. In an atmosphere well mixed by convection, directional changes in the boundary layer are small, see Meteorological Office (1975).

The view that wind veers with increasing strength was initially supported by Giblett (1932) who measured changes in wind speed and direction over a period of 10–30 minutes. Giblett's period is not representative of the time-scale associated with gusts. The chosen period of between 10 and 30 minutes is within the spectral gap of the power spectrum representing surface wind speeds reported by van der Hovan (1957) and Ishida (1989), i.e. the region of little fluctuating wind speed. However, these results do not rule out the possibility that fluctuations do occur on some occasions. Lemone (1973) found fluctuating wind speeds of a period of 30 minutes associated with mesoscale convection. Brettle (1990) using 30-second averages of speed and direction came to the conclusion that wind veering in gusts could not be relied upon by mariners. Hisscott and Roberts (1991) using an independent method to Brettle found no evidence to support wind veering in gusts.

2. Data and site

The data were collected at the Meteorological Office Research Unit at Cardington. The horizontal (u, v) and vertical (w) components of the wind were measured with sonic anemometers 6 m and 20 m above the ground. The data were collected digitally with sampling at 20 Hz and 10 Hz respectively during near neutral and unstable conditions. Table I shows the basic statistics of the data set. Each set is 30 or 40 minutes long. There were no significant trends in the time-series of wind speeds over the recording duration. The 6 July 1990 and 19 June 1990 data sets were both filtered using a 1-second block average in order to remove the highest frequencies. A 10-second block average filter was applied to the 19 June 1990 data set to analyse longer-duration gusts. L = Monin–Obhukov length defined as

$$L = -\frac{u_*^3 T_a}{kg\overline{w'T'}}$$

where u_* is the friction velocity, k von Kärmän's constant, g acceleration due to gravity, T_a the absolute temperature, $\overline{w'T'}$ is the surface temperature flux and σ_s is the standard deviation of the horizontal wind. Estimates of L show that the 6 July 1990 data set is near neutral whilst the 19 June 1990 data set is slightly unstable. The area around Cardington is generally very flat: The local roughness length at the anemometer site is about 0.01 m; the area average roughness length is around 0.1 m, typical of land with fields, hedges and occasional trees.

3. Gust definition

The definition of a gust and a lull used was taken to be an increase or decrease in wind speed to an amplitude which was at least 1 σ away from the mean wind speed. The speed s and direction θ of the gust were calculated from the u, v components making up the gust where $s = \sqrt{(u^2 + v^2)}$ and $\theta = \arctan(v/u)$, the direction being measured relative to the mean wind direction. The duration of the gust was defined as the time taken for the gust to reach an amplitude and return to a minimum, usually taken to be a return to the mean wind. A similar definition was used by Bergström (1987) in analysing statistical characteristics of gusts.

4. The von Mises distribution function

In meteorology, wind direction measurements are based on angular measures defined on the circle. It is often tempting to use linear estimates of the mean,

Table I. Summary of Cardington data used, see text for explanation of symbols

Date (1990)	Start time (UTC)	Duration (min)	z (m)	$\bar{U}$ (m s^{-1})	σ_s (m s^{-1})	L (m)
6 July	1130	30	6	7.4	1.3	−250
"	1200	30	6	7.6	1.3	−182
"	1230	30	6	6.7	1.5	−286
"	1300	30	6	7.7	1.3	−250
"	1330	30	6	7.9	1.5	−200
"	1400	30	6	6.5	1.8	−158
19 June	1218	40	20	8.1	1.4	−63
"	1436	40	20	7.4	1.4	−79
"	1528	40	20	6.8	1.5	−94
"	1618	40	20	6.6	1.1	−47

though this is clearly erroneous as the following example illustrates. Let there be two measured angles 1° and 359° respectively, then the linear mean would give 180° which is absurd. The example given, though extreme, illustrates that when dealing with directional data it is more appropriate to use statistical measures defined on the circle rather than on the line. The data presented in this paper are directional and are best represented by a probability density function defined on the circle. A widely used model for directional data is the von Mises distribution function, first introduced by von Mises in 1981 when investigating whether atomic weights were integers. The von Mises probability density function is defined by the equation,

$$M(\theta, \mu, \kappa) = \frac{1}{2\pi I_0(\kappa)} \exp^{\kappa \cos(\theta - \mu)} \qquad (1)$$

where $I_0(\kappa)$ is the modified Bessel function of the first kind and order zero defined by

$$I_0(\kappa) = \frac{1}{2\pi} \int_0^{2\pi} \exp^{\kappa \cos\theta} d\theta = \frac{1}{\pi} \int_0^{\pi} \exp^{\kappa \cos\theta} d\theta,$$

μ is the location point, κ the concentration parameter. The distribution function is analogous to Gauss's normal distribution function defined on the line. The location point behaves like a mean, being the point around which the wind direction tends to congregate. The concentration parameter corresponds to a variance about the mean wind direction. If the value of κ is large then the distribution function is highly concentrated about μ. The maximum likelihood estimates, $\hat{\mu}$ and $\hat{\kappa}$, of μ and κ are determined as follows. Let

$$\overline{\sin\theta} = \frac{1}{n} \sum_{i=1}^{n} \sin\theta_i, \overline{\cos\theta} = \frac{1}{n} \sum_{i=1}^{n} \cos\theta_i$$

then

$$\hat{\mu} = \arctan\left(\frac{\overline{\sin\theta}}{\overline{\cos\theta}}\right), R = \surd\{(\overline{\sin\theta})^2 + (\overline{\cos\theta})^2\}.$$

R is the length of the resultant, $\overline{OP}$, of a point P ($\cos\theta_i$, $\sin\theta_i$), $i = 1, \ldots, n$, defined on the circle, centre O. The value of $\hat{\kappa}$ corresponding to R is determined from a table such as that given by Mardia (1972). The fitting of the von Mises Probability Density Function (PDF) to the actual data can be tested by using the goodness-of-fit test (chi-square) defined by

$$\chi^2 = \sum \frac{(A - E)^2}{E} \qquad (2)$$

where A is the actual frequency of events occurring within a bin width of size 10 or 15° and E is the expected frequency of events occurring within the bin width. E is calculated by integrating the PDF from equation (1) across the size of the bin width and then multiplying the integrated function by the total number of observations. In using equation (2) care must be exercised because the χ^2 distribution is only an approximation to the exact distribution of the quantity represented by the equation. It is known that E in each bin width should be greater or equal to 3 for the approximation to be valid. This is why the above bin widths have the range shown in Tables II–IV in order to ensure that the number of events in each bin width is large. The number of degrees of freedom is defined as the total number of bin widths minus the number of parameters in the PDF estimated from the data. Hypothesis testing is employed in order to ascertain whether there is a significant veering or backing. If μ is constrained to be zero in the PDF then the PDF will be symmetric about zero, which means there is no preferred direction. If μ is not constrained to be zero then the PDF will not be symmetric about zero and a preferred direction will be evident. From these two distribution functions, and from the difference between their χ^2 distributions, it is possible to test whether there is evidence for asymmetry in the distribution functions. For large samples the difference is distributed approximately as χ_1^2 (chi-square distribution of one degree of freedom). This property enables a goodness-of-fit test for the hypothesis that $\mu = 0$.

$$\chi^2_{\hat{\mu}=0} - \chi^2_{\hat{\mu}>0} = \chi^2_1. \qquad (3)$$

Equation (3) comes from the mathematical theory of statistics. For a more detailed theoretical treatment the reader is referred to Silvey (1975) and Plackett (1971). Equation (3) describes the goodness-of-fit test where an extra constraint has been imposed on the distribution function by setting $\hat{\mu} = 0$. If $\chi^2_{\hat{\mu}=0} - \chi^2_{\hat{\mu}>0} > \chi^2_1$ then the hypothesis $\mu = 0$ is rejected. If $\chi^2_{\hat{\mu}=0} - \chi^2_{\hat{\mu}>0} < \chi^2_1$ then the hypothesis $\mu = 0$ is accepted. This does not mean that the distribution is symmetric, simply that there is no (or not enough) evidence for asymmetry.

5. Data analysis

The total number of gusts defined in the time-series for the 6 July 1990 using the 1-second filter was 198 out of a total time period of 3.0 hours. 58% of the gusts show backing whilst 42% show veering. The following distributional estimates were found using the procedure outlined in section 4: $\hat{\mu} = 1.9508$ and $R = 0.9815$. For $R = 0.98$, $\hat{\kappa} = 25.2522$ and for $R = 0.99$, $\hat{\kappa} = 50.242$, and by linear interpolation the maximum likelihood estimate of $\hat{\kappa}$ is 29.00. Table II shows the expected frequency calculated from the von Mises PDF against the actual frequency of gusts and lulls. It can be seen that the von Mises PDF fits well to the real data.

The data set obtained on the 19 June 1990 was similarly analysed. The number of gusts in this time-series was 129 with 58% veering and 42% backing which is opposite to what was found in the first data set. For the lulls there were a total number of 109 with 55% backing and 45% veering again opposite to the first data set. The distributional estimates were obtained as above

Table II. Expected and actual frequencies for a 1-second block average on 6 July 1990, using von Mises probability density function

Bin range	Gusts: $\hat{\kappa} = 29$, $\hat{\mu} = 1.95$		Bin range	Lulls: $\hat{\kappa} = 21.0$, $\hat{\mu} = -2.91$	
	Frequencies			Frequencies	
	Actual	Expected		Actual	Expected
0–10	66	66.51	0–10	34	36.56
10–20	40	35.93	10–180	25	21.87
20–180	8	10.36	−(0–10)	40	43.59
−(0–10)	54	57.29	−(10–20)	36	28.40
−(10–20)	22	23.04	−(20–180)	8	12.57
−(20–180)	8	4.84			

Table III. As Table II but for 19 June 1990

Bin range	Gusts: $\hat{\kappa} = 18.2$, $\hat{\mu} = -2.591$		Bin range	Lulls: $\hat{\kappa} = 20.0$, $\hat{\mu} = 2.74$	
	Frequencies			Frequencies	
	Actual	Expected		Actual	Expected
0–10	35	31.94	0–15	40	44.99
10–20	12	16.50	15–180	19	18.67
20–180	5	6.26	−(0–15)	39	36.03
−(0–10)	38	36.62	−(15–180)	11	9.29
−(10–20)	29	24.78			
−(20–180)	10	12.88			

Table IV. As Table III but for 10-second block averages

Bin range	Gusts: $\hat{\kappa} = 45.0$, $\hat{\mu} = 3.53$		Bin range	Lulls: $\hat{\kappa} = 17.5$, $\hat{\mu} = 2.56$	
	Frequencies			Frequencies	
	Actual	Expected		Actual	Expected
0–10	14	12.15	0–15	17	17.14
10–180	3	2.48	15–180	8	8.09
−(0–10)	17	17.70	−(0–15)	11	14.25
−(10–180)	9	9.68	−(15–180)	8	4.51

and are contained in Table III for 1-second average data.

A 10-second block average filter was also applied to this particular data set in order to examine the longer duration gusts. Table IV shows the resulting actual frequencies against the expected frequencies for the gusts and lulls. Table V shows the statistical results. The goodness of fit between the actual and expected frequencies can be tested using equation (2), noting that (from look-up tables) $\chi^2_1 = 3.841$.

The statistics show that there are gusts and lulls which may either back or veer, and in the last three cases there is no preferred sense in unstable conditions. Thus, the evidence for a preferred direction when such an event occurs is inconclusive, and is not supportive of the wind veering in gusty conditions. The behaviour would seem to indicate randomness.

6. Conclusion

The data set recorded on the 6 July 1990 suggested an asymmetry in the gust and lull frequency distribution functions opposite to the sense that one might expect, though the asymmetry present in both cases is weak. The second data set recorded on the 19 June 1990 has an asymmetrical gust distribution function but in the case of lulls there is no evidence to suggest an asymmetry. In the case of longer-duration gusts there is no evidence for an asymmetry in the gust and lull frequency distribu-

Table V. Statistical results, where G = gust, L = lull, B = backing, V = veering, NP = no performance, N = neutral, U = unstable, A = accepted and R = rejected.

G or L	Table	$\chi^2_{\hat{\mu}>0}$	$\chi^2_{\hat{\mu}=0}$	$\chi^2_{\hat{\mu}=0} - \chi^2_{\hat{\mu}>0}$	$\hat{\mu} = 0$	Sense	Stability
G	II	3.302	7.330	4.028	R	B	N
L		4.616	10.450	5.834	R	V	N
G	III	3.165	9.245	6.080	R	V	U
L		1.119	2.970	1.851	A	NP	U
G	IV	0.597	4.080	3.482	A	NP	U
L		3.462	3.841	0.378	A	NP	U

tions. The deviations from symmetry when they occur are only slight and are not significant enough to establish that the wind veers or backs in gusts. These results are very suggestive of random incidence of veering or backing in neutral or convective conditions. Although only one longer time-scale was examined there is no evidence to suggest that different results will be found for longer time-scales. The reproducibility of the fitting of the von Mises PDF to meteorological wind data which is directional in nature is also noted in all cases used in the analysis.

Acknowledgements

I would like to express my thanks to the following colleagues for their useful dialogue. R. Maryon for meteorological discussion and comments which have led to the improvement of the presentation of the paper. A. Grant for meteorological discussion and supplying the 6 July 1990 data set. Dr P. Hignett for supplying the 19 June 1990 data set. Dr M. Farrow for discussion on mathematical properties of the von Mises PDF.

References

Bergström, H., 1987: A statistical analysis of gust characteristics. *Boundary-Layer Meteorol*, **39**, 153–173.

Brettle, M.J., 1990: Wind direction and gusts. *Weather*, **45**, 373–375.

Giblett, M.A., 1932: The structure of wind over level country. *Geophys Mem, Meteorol Off*, No. 54.

Hisscott, C.A. and Roberts, A.P., 1991: Wind direction and gusts at Ronaldsway. *Weather*, **46**, 215–216.

Ishida, H., 1989: Spectra of surface wind speed and air temperature over the ocean in the mesoscale frequency range in JASIN-1978. *Boundary-Layer Meteorol*, **47**, 71–84.

Kristensen, L., 1989: In search of a gust definition. RisøNational Laboratory, Risø-M-2796.

Lemone, M.A., 1973: The structure and dynamics of horizontal roll vortices in the planetary boundary layer. *J Atmos Sci*, **30**, 1077–1091.

Mardia, K., 1972: Statistics of directional data. London, New York, Academic Press.

Meteorological Office, 1967: Meteorology for mariners. London, HMSO.

—, 1971: Handbook of aviation meteorology. London, HMSO.

—, 1975: Handbook of weather forecasting. (Unpublished, copy available in the National Meteorological Library, Brascknell.)

Plackett, R.L., 1971: An introduction to the theory of statistics. Edinburgh, Oliver and Boyd.

Silvey, S.D., 1975: Monographs on statistics and applied probability 7. Chapman and Hall.

van der Hovan, I., 1957: Power spectrum of horizontal wind in the frequency range 0.00007 to 900 cycles per hour. *J Meteorol*, **14**, 160–164.

551.506.1(41-4)

The winter of 1990/91 in the United Kingdom

G.P. Northcott
Meteorological Office, Bracknell

Summary

The winter of 1990/91 was generally cold and, in most areas, wet; many areas had more sunshine than usual, although it remained dull over part of north-west Scotland.

1. The winter as a whole

Mean temperatures over the winter season were below normal nearly everywhere, apart from Shetland, Orkney and the Isle of Lewis, ranging from 0.4 °C above normal at Lerwick, Shetland to 1.6 °C below normal at Fowey, Cornwall. Rainfall amounts over the winter period were above normal in western and southern Scotland, but below normal in Orkney, Shetland, eastern Scotland and Northern Ireland; much of England and Wales was wet, with the notable exception of the Merseyside and Greater Manchester areas, parts of Lincolnshire and East Anglia, and the southern coastal counties from Cornwall to Kent. Amounts ranged from nearly 179% at Kielder Castle, Northumberland to 68% at Manston, Kent. Sunshine amounts were about normal over Scotland as a whole, although part of north-west Scotland had a very dull winter, and generally above normal over England, Wales and Northern Ireland, and ranged from 187% of average at Buxton, Derbyshire to as little as 55% of average at Kinlochewe, Highland Region.

Information about the temperature, rainfall and sunshine during the period from December 1990 to February 1991 is given in Fig. 1 and Table I.

2. The individual months

December. Mean monthly temperatures were generally about normal for the month, and ranged from 0.8 °C above normal at Fyvie Castle, Borders Region to 1.4 °C below normal at Fowey, Cornwall. Brooms Barn, Suffolk reported the coldest December since 1982. Monthly rainfall totals were generally above normal in the north and west and below normal in the south and east, with nearly twice the average in parts of southern Scotland and northern England but only just over half the average on the south coast. Monthly sunshine amounts were generally above average except for parts of western Wales, eastern England and central areas of Scotland, ranging from more than 180% at Belfast Airport to 61% in the Edinburgh area.

On the 7th and 8th snowfall was very heavy over northern England, Wales, the Midlands and south-west England, with heavy drifting in gale-force winds, causing considerable disruption to traffic of all sorts and cutting power lines. The snow did not freeze, however, but melted very rapidly during the next few days, as the temperature rose a little. On the 11th and 12th storm-force winds swept down the North Sea; Fair Isle, Shetland had a gust to 73 kn. From the 23rd until the

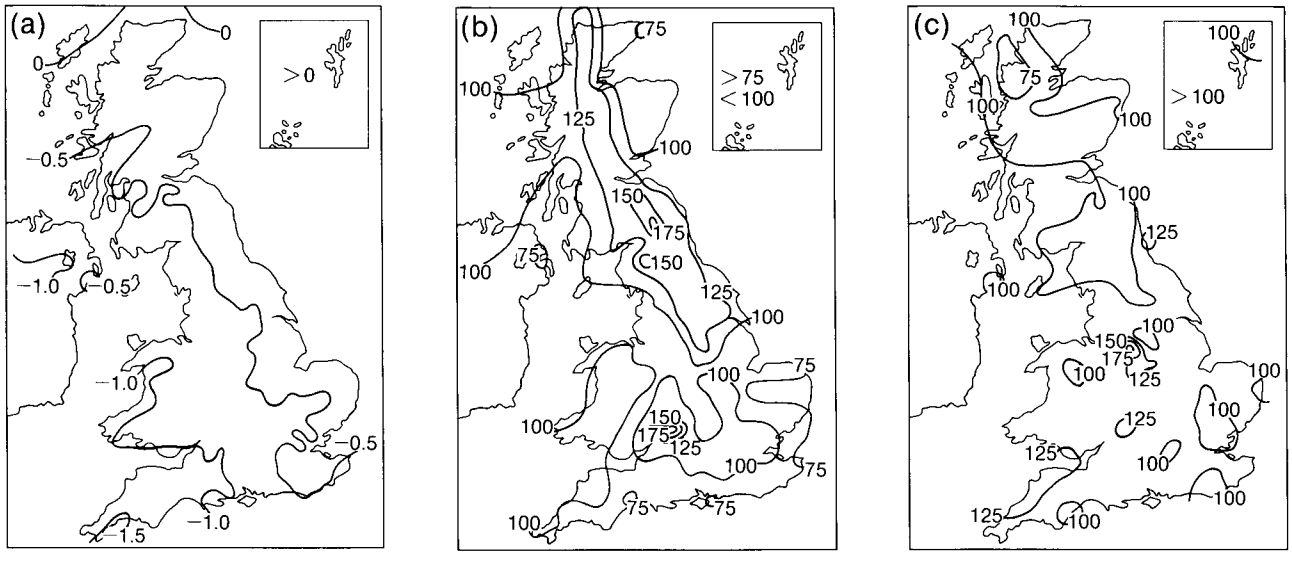

Figure 1. Values of (a) mean temperature difference (°C), (b) rainfall percentage and (c) sunshine percentage for winter, 1990/91 (December–February) relative to 1951–80 averages.

Table I. District values for the period December 1990–February 1991, relative to 1951–80 averages

District	Mean temperature (°C)	Rain-days	Rainfall	Sunshine
	Difference from average		Percentage of average	
Northern Scotland	−0.1	−1	96	98
Eastern Scotland	−0.3	−2	112	104
Eastern and north-east England	−0.3	0	128	104
East Anglia	−0.6	−2	88	107
Midland counties	−0.8	−1	100	112
South-east and central southern England	−0.7	−1	98	108
Western Scotland	−0.6	−1	104	100
North-west England and North Wales	−1.0	−2	110	113
South-west England and South Wales	−1.4	−2	101	121
Northern Ireland	−0.7	−2	90	122
Scotland	−0.3	−2	102	101
England and Wales	−0.7	−1	105	111

Highest maximum: 14.8 °C in Midland counties in February.
Lowest minimum: −14.8 °C in western Scotland, also in February.

end of the month very strong winds and bands of rain, often prolonged and heavy at times, crossed many parts. On the 25th and 26th gales and storm-force winds affected many areas. Gusts of more than 70 kn were reported at Greenock Port, Strathclyde Region, Langdon Bay, Kent, Camborne, Cornwall, Plymouth, Devon and Killough and Orlock Head in Northern Ireland and on the 25th there were reports of tornadoes over Devon, Somerset and Avon. Sleet and snow were reported as far south as South Wales on the 27th and Towy Castle, Dyfed reported hailstones of 15 mm diameter. On the 29th a whirlwind caused extensive damage to houses in Gorseinon, South Wales, and a cottage in North Wales was hit by lightning. Towy Castle reported a whirlwind crossing the station with a maximum height of 35 m at 11 h on the 30th.

January. Mean monthly temperatures were above normal in northern Scotland and central and south-eastern England including East Anglia, and below normal elsewhere, ranging from 1.5 °C above normal at Bexhill, East Sussex to 1.5 °C below normal at the Lizard, Cornwall. Monthly rainfall totals were above normal everywhere, except in eastern Scotland, the Western Isles, East Anglia, and in northern and eastern England; the area around Aberdeen had about 30% of normal and nearby Fyvie Castle had as little as 20% of normal. In contrast Ardtalnaig, Tayside Region and Newton Rigg, Cumbria had more than 160% of normal rainfall. Over Northern Ireland as a whole it was the driest January since 1972. Monthly sunshine amounts were above average nearly everywhere, although it was rather dull over much of western and south-western Scotland, and ranged from 202% of average at Tynemouth, Tyne and Wear to as little as 69% of average at Kinlochewe, Highland Region. It was the sunniest January over Northern Ireland since 1959 and at Wick, Highland Region since records began there in 1946.

The weather was frequently stormy during the first week, with strong winds, rain and snow, and long sunny periods in between. On the 1st, periods of heavy rain aggravated by rapidly melting snow caused flooding in many areas of southern Scotland. On the 5th, gales coupled with high tides caused extensive and costly damage to parts of western and southern coasts from Strathclyde to Sussex, as the sea breached defences. There was considerable flooding in many areas and disruption to power supplies and transport, especially in the west. After the 10th the month was generally dry, although there was rain in many places between the 17th and 20th, and snow in some western areas on the 30th and 31st. Thundery outbreaks were frequent and widespread between the 3rd and 7th. There were isolated reports of thunder on the 9th and 10th and a broad area of thundery activity over south-east England on the 11th.

February. Mean monthly temperatures were below normal nearly everywhere and ranged from 0.1 °C above normal at Lerwick, Shetland to 3.1 °C below normal at Greenwich, Greater London. Monthly rainfall totals were above normal in most parts of eastern Scotland and eastern England and generally below normal elsewhere, ranging from 187% at Durham to as little as 36% at Fort William, Highland Region. Monthly sunshine amounts were generally above average in western areas and below average on eastern coasts, ranging from 142% at Tiree, Strathclyde to 62% at Boulmer, Northumberland.

February was unsettled throughout, with cold weather and frequent falls of snow during the first half. Some sleet or snow showers fell during the first five days of the month. Between the 6th and 14th snowfall was heavy in many places and it became very cold for a few days. On the 6th many parts had snow showers during the day, especially in the east: Anvil Green, Kent reported 6 cm of snow lying. Snow showers over the North Downs

overnight gave a cover in most areas by the morning of the 7th; later that day up to 14 cm of level snow lay in some places. During the following night falls of snow over England and Wales, heavy at times, gave up to 20 cm in places as far apart as Essex, mid Wales and Yorkshire. Depths were very variable, however, with 47 cm at Wilsden, West Yorkshire, 35 cm at Pencelli, Powys and 20 cm at St James's Park, central London, probably the greatest depth in London since the end of December 1962. On the 9th some areas had heavy snowfall; some notable depths included 51 cm at Wilsden, 35 cm at Pencelli and 30 cm at Honington, Suffolk; over the next few days snow depths included 45 cm at Fylingdales, North Yorkshire on the 12th, 46 cm at Longframlington, Northumberland on the 13th, and 15 cm at East Hoathly, East Sussex on the 14th. After mid month it became somewhat milder, although remaining generally wet and at times windy. On the 8th there was some thundery activity over eastern parts of England. A thunderstorm was reported to the west of London during the 27th.

551.593.653(4).551.506.1

Noctilucent clouds over western Europe during 1990

D.M. Gavine
29, Coillesdene Crescent, Edinburgh EH15 2JJ

Summary

Noctilucent cloud observations by voluntary and professional observers in the British Isles, Denmark and The Netherlands suggest a lower incidence of the phenomenon than in recent years.

Table I summarizes the noctilucent cloud (NLC) reported to the Aurora Section of the British Astronomical Association (BAA) during 1990. The times (UT) are the reported sightings, not necessarily the duration of a display. 'Negative' nights (Table II) are based on the judgement of two or more experienced observers north of 54°N with clear or nearly clear sky conditions over the period of the night when NLC is likely to occur.

Table I. Displays of noctilucent clouds over western Europe during 1990

Date — night of	Times UT	Notes
22/23 May	2135–2310	Bands, billows and whirls at Chelmsford, Reading and Godalming; NLC at Rotterdam; faint structures visible in Denmark — suspected auroral light with NLC at Vildbjerg 2230–2310, and at Kemnay near Aberdeen.
23/24	2229–2300	Faint bands at elev. 16°, Vildbjerg; no NLC in clear sky in Scotland and I. of Man.
24/25		Suspected faint NLC at Ronaldsway but no NLC in clear sky in Scotland and Morpeth.
25/26	2345–0130	Moderately bright veil and bands to elev. 12° at Vildbjerg, greenish NLC in dawn sky at Rotterdam. No NLC in Scotland and Morpeth.
2/3 June	0000–0200	Suspect faint NLC at Kemnay. No NLC at Edinburgh and Morpeth.
7/8	0240	Suspect billows to elev. 45° at Upton on Severn.
12/13 June	2300	'Silvery' NLC in NW to elev. 40°, Co. Clare, aurora observed at Rønne, Bornholm.
17/18	2240	Moderately bright bands in tropospheric cloud breaks at Rønne.
19/20	2140–0230	Moderately bright and extensive display, all forms, described by 16 observers from Kirkwall to London. Maximum elevs 70° (Alness), 56° (Morpeth), 40° (Upton), 10° (Witham, Essex).
22/23	2110–2150	Suspect bands and patches at Upton. No NLC in I. of Man or in Scotland 2230–2300.
23/24	2130–0115	Faint bands, billows and patches visible in binoculars at Morpeth and Upton. No NLC at Rønne or in Scotland 2305–0030.
24/25	0020–0115	No NLC up to 0000. Faint bands in Ayrshire, very faint NLC at Morpeth.

Date — night of	Times UT	Notes
27/28 June	0005–0130	No NLC before 0000. Very faint bands, slight billows, Ayrshire, Machrihanish and Edinburgh.
28/29	0100–0200	Faint bands at Dundee and Aberfeldy. No NLC at Alness 2315.
29/30	2200–2330	Faint bands and whirls to elev. 9°, Vildbjerg. No NLC visible at Rønne.
30/01	2100–2130	Bands and billows to elev. 15°, Rotterdam.
2/3 July	2300	Moderately bright bands reported at Aberfeldy but NLC reported absent at Machrihanish, Milngavie and I. of Man.
3/4	2315–0000	Faint bands at elev. 6°, Rønne.
7/8		Positive NLC sighting at Kemnay, no details.
8/9	2330–0130	Faint bands in trop. cloud at Morpeth, NLC at Kemnay. No NLC at Rønne but very faint bands visible in binoculars at Vildbjerg.
10/11	2120–0145	Fairly bright display, all forms, visible from Kinloss to Chichester, and Wadebridge, Cornwall. Max. elev. at Morpeth 24°. Photographed by Mr Trafford at Cambridge. 'Chaotic' silvery-blue NLC at De Bilt, bands and billows at Rotterdam and Deventer.
11/12	2156	Very faint bands visible in binoculars, Vildbjerg. No NLC at Morpeth and I. of Man.
14/15	2350	Small faint NLC patch reported at Stirling but negative reports from 3 other Scottish stations, Morpeth and Rønne.
16/17	2240–0240	Moderately bright veil, bands, billows and patches at Wick (elev. 22°), Kinloss, Ayrshire and Pensarn (N. Wales). No NLC in Scotland before 2345.
17/18 July	2200–0320	Fairly faint veil, bands, billows and patches from Wick to N. Wales. NLC in zenith at Carlisle 2200.
19/20	2200–0030	Fairly faint bands, billows and whirls to elev. 11° at Vildbjerg, NLC reported 0030 to dawn by MV *Selectivity* in Kiel Canal. Faint bands suspected near zenith in Carlisle 2200 but no NLC reported in I. of Man.
21/22	2115–2245	No NLC in Scotland 2200–0000. Faint veil at Wick and Morpeth, faint patches at Carlisle. No NLC at I. of Man.
23/24	2025–2215	No NLC in Scotland, I. of Man or Morpeth. Dr Smeaton observed NLC at Helsinki.
24/25	2300	Faint veil at Alness. No NLC at Morpeth or I. of Man. Mr Trafford observed NLC at Helsinki 2100.
25/26	2130–0115	Faint bands, billows and whirls at Vildbjerg elev. 9°, to 2330. MV *Selectivity* at 56° 47'N, 12°E reports bands at elev. 40°, 0045–0115. No NLC at I. of Man and Machrihanish.
26/27	2145–0250	Bright bands and patches at Kinloss and Alness, described as intense electric-blue, photographed by Mr Fraser. No NLC at Rønne but faint bands at Vildbjerg and MV *Selectivity* in the Baltic. Drs Fischer and Hombich photographed very bright horizontal bands with aurora above from Baltic ferry at lat. 59°N.
31/Aug 1	2055–2325	Very faint veil, bands and billows visible in binoculars at elev. 6° at Vildbjerg. No NLC at Rønne.

Table II. Negative nights (British Isles) north of latitude 54° N

May 18/19; 19/20; 20/21; 26/27; 27/28; June 1/2; 3/4; 5/6; 13/14; 14/15; 18/19; 20/21; 21/22; July 5/6; 18/19; 20/21; 22/23; 28/29 (aurora), 30/31; Aug. 1/2.

Despite many clear nights there were 25 positive and 6 suspected sightings, a lower incidence than in recent years. Of these, only 4 displays were noteworthy, many were very faint, some were found only by a binocular search by dedicated amateur observers.

Contributions were received from 27 individual observers and 5 meteorological stations in the United Kingdom, 3 stations of the Royal Netherlands Meteorological Institute, 3 observers in Denmark, 1 in Eire and 1 UK observing vessel. Again, the superb photography by Mr Olesen and Mr Andersen of Denmark has enhanced BAA meetings and exhibitions. Details of Finnish-Estonian NLC sightings are not now mentioned here, but are published annually in the journal *Ursa Minor* of the URSA Astronomical Association (Laivanvarustajankatu 3, SF-00140 Helsinki 14).

As before, the intention of the BAA Aurora Section is to provide a data bank in both aurora and NLC for professional workers. Details of individual NLC nights are available from the author, but all NLC data up to 1988 are held in the Balfour Stewart Archive at the University of Aberdeen.

Our thanks to all observers, amateur and professional (we would like to encourage more professional input into the survey), and to Mr Ron Livesey, Director of the BAA Aurora Section, Mr Tom McEwan, Director of the Junior Astronomical Society Aurora Section, Mr V. Mäkelä (Finland), Dr B. Zwart (The Netherlands), Mr M. Zalcik (USA–Canada NLC Network), and Dr M. Gadsden (University of Aberdeen).

Correction

Meteorological Magazine, September 1991, p. 168, Table III.

The heading above the years should read 'Effective precipitation' and not 'Soil moisture deficit'.

Reviews

Principles of air pollution meteorology, by T.J. Lyons and W.D. Scott. 157 mm × 235 mm, pp. vi+224, *illus.* London, Belhaven, 1990. Price £25.00. ISBN 1 85293 079 9.

This very readable book is a very useful addition to the library of anyone concerned with air pollution. The text covers a wide range of relevant topic-areas: the nature of the atmospheric boundary layer, diffusion theory, the chemical and physical properties of pollutants, the techniques of monitoring and the impact of pollution on crops and the environment. It ends with brief descriptions of many current commercially available computer models developed mainly in the USA.

However, being only some 200 pages long one cannot expect, and one does not get, anything like a complete cover of all these topics. What you do get is a useful 'flavour' of the subject, a background which will be helpful in reading other more up-to-date and specialized papers and books. The authors develop some aspects within each area, giving them fullish treatment, whilst other aspects are glossed over rather more hurriedly. For example, the section on atmospheric diffusion goes into *K*-theory in some detail, but gives too little emphasis (if any) to higher-order closure schemes, to similarity theory or random-walk techniques and allied methods which are much more widely used these days than *K*-theory. There is also little discussion on modern perceptions of dispersion in convective conditions or on gravity flows at night. The effects of complex terrain on dispersion and rain-out from precipitating clouds are not mentioned. These are all important matters.

But I do not wish to damn the book; on the contrary it has many good points, many points are very well explained and overall the book gives a very helpful introduction provided the reader goes on to read other texts. It is very readable, you can dive in almost anywhere and quickly pick up and understand the message, a virtue that is to be highly commended! The book is nicely produced with clear text and good diagrams, with very few typographical errors, and all at a sensible price.

F.B. Smith

Impact models to assess regional acidification, edited by J. Kämäri. 162 mm × 245 mm, pp. xvi+310, *illus.* Dordrecht, Kluwer Academic Publishers, 1990. Price Dfl.195.00, US$115.00. £71.50. ISBN 0 7923 0710 0.

When summoned to meetings at the National Radiological Protection Board at Harwell, I frequently drive across country from Theale to East Ilsley, saving miles and gaining solitude from the quiet leafy lanes of Berkshire. Over the last few years, however, the journey has been tinged by sadness at seeing so many once-splendid beech trees slowly dying, their leaves turning a sickly yellow long before the autumn frosts bring natural colouring to our woodlands.

I feel some guilt too, since my car's exhaust gases are adding their small share to the acidification of the land, which in part may be the cause of the sorry state of the beeches that once ennobled the surrounding landscape.

Questions race through my mind as I drive: just how much pollution can the land take before it really begins to suffer? Are we already overloading the soil and will devastation become increasingly apparent across the land as the years go by? When and where and by how much do we need to reduce emissions? What will be the cost? ...

For 20 years scientists have been trying to come to terms with acidification problems. At first the emphasis was on trying to discover the extent and rate of acidic deposition. Then came attempts to model the complex processes taking place within the atmosphere from emissions, through transport and dispersion, through complex chemical changes, and eventually through removal processes leading to deposition. At the same time others have been studying the effects of acidic depositions on soils, trees, waters, fish and other wildlife. Much has been learnt. The concept of critical loads has been proposed — the idea that any area can cope with long-term depositions up to some critical level above which serious damage to the environment will occur. Due to many spatially varying factors the critical loads can be expected to vary from one area to another. Work has also started on so-called emission abatement strategies whereby over a large area like Europe emission–deposition relationships are studied so that emissions may be 'intelligently' reduced in those areas where the benefit to the environment as a whole will be greatest, taking into special account areas where current loads exceed their critical loads.

This brings me to the book under review. It contains 14 papers either presented during, or written as a result of, a Task Force Meeting on 'environmental impact models designed to assess regional acidification' held in 1987 in Warsaw. The papers have been brought together in this useful and nicely produced volume by Juha Kämäri, one of the organizers of the meeting.

Although not of great direct meteorological interest, the book does provide much useful information con-

cerning the topics outlined above, and in so doing has considerable bearing on the development of environmentally orientated meteorological transport and deposition models. The book should therefore find its place in all meteorological libraries where such models are developed.

F.B. Smith

A field test of thermometer screens, by T. Andersson and I. Mattisson. 209 mm × 296 mm, pp. 40, *illus.* Norrköping, Sweden, SMHI, 1991. ISSN 0347 2116.

This gives results from an 11-month-long experiment comparing the performance of three standard SMHI 'Stevenson' screens with that of five smaller commercial screens (the Vaisala, Young, Lambrecht...on ordinary and long poles...also the Teledyne). One Stevenson screen was small (40 cm × 40 cm × 68 cm); the other two were large (70 cm × 53 cm × 81 cm), one having clean white louvres while the other was older and deliberately left in 'bad' condition with some paint having flaked off, leaving bare wood in places.

The 'Teledyne 327B' is motor-aspirated (and may be regarded as a development of the Assman psychrometer). In the opinion of the authors, it was taken as the reference for this experiment 'to get as good an estimate as possible of the air temperature', but that premise calls into question the validity of the American manufacturer's (1984) claims for accuracy and performance of the ventilated Teledyne, which appear to have been merely presented at face value (as Appendix 1) where engineering drawings would have helped an appreciation of the instrument, not to mention prior testing and results.

One difficulty with taking a ventilated instrument as the standard reference (against which non-aspirated thermometers are compared) concerns probable artificiality of the temperature where naturally stagnating air is forced into motion during calm conditions. Aspirated entrainment of air from non-standard heights above ground level could have produced the large differentials (of 2–3 °C) recorded on 13 December 1989, a day of clear skies, light winds and a snow cover...see p. 10. Other situations of (1) strong temperature inversion or (2) rapid lapse rate changes (e.g. during showers) were found to produce large differentials of between 3 and 3.5 °C (e.g. on 28 June 1989).

This latter situation, of summertime showers producing sudden cooling of surfaces appeared to show a pronounced 3 °C 'lag' of temperatures recorded by the large 'Stevenson' screen in bad condition. Alternatively, it could be argued that some of the instruments in the smaller, novel screens read too low because they did not shield their thermometers well enough! This is because, to some extent, the temperature of the enclosure surfaces (aluminium in the case of the Lambrecht's) is being measured. Nevertheless, solar heating from received radiation was more-efficiently absorbed, stored, and re-radiated by the bare wooden patches on the older 'Stevenson' and the moral to observers is that screens should not be allowed to fall into neglect — temperature discrepancies will result if louvres are not kept clean and white.

Despite the rather-limited test period (from April 1989 to February 1990) which included a relatively mild winter in Sweden, some interesting comparisons were made by continuous monitoring in various weather conditions, and the results are well presented. However, the basic purpose of a thermometer screen is to isolate its instruments from ambient radiative surfaces, and this commendable experiment has shown that some of the smaller commercial screens do not achieve this because they are influenced by the materials of which they are made.

The difficulties in keeping roadside 'Stevenson' screens in good condition are noted and, one hopes, more-modern construction techniques may allow improvements (such as white plastic lamination of the wooden louvre surface) in their manufacture.

W.S. Pike

Books received

The listing of books under this heading does not preclude a review in the Meteorological Magazine at a later date.

Satellite remote sensing in climatology, by A.M. Carleton (London, Belhaven Press, 1991. £39.50) emphasizes the contribution of satellite data to climate theory. Also emphasized is the monitoring of possible human impacts on the climate system. ISBN 1 85293 039 X.

Fractals: endlessly repeated geometrical figures, by H. Lauwerier (London, Penguin Books, 1991) explains the basic mathematics of fractals, and is intended for a wide audience. Constructing fractals with computer programs (answers in the back) is included. ISBN 0 14 014411 0.

Mid-latitude weather systems, by T.N. Carlson (London, Routledge, 1991. £75.00 (hardback), £19.95 (softback)) attempts to present a fusion of synoptic and dynamic meteorology. Conventional weather charts together with equations are used to illustrate the evolutions of weather patterns. ISBN 0 04 551115 2, 0 04 551116 0.

GUIDE TO AUTHORS

Content

Articles on all aspects of meteorology are welcomed, particularly those which describe results of research in applied meteorology or the development of practical forecasting techniques.

Preparation and submission of articles

Articles, which must be in English, should be typed, double-spaced with wide margins, on one side only of A4-size paper. Tables, references and figure captions should be typed separately. Spelling should conform to the preferred spelling in the *Concise Oxford Dictionary* (latest edition). Articles prepared on floppy disk (IBM-compatible) can be labour-saving, but only a print-out should be submitted in the first instance.

References should be made using the Harvard system (author/date) and full details should be given at the end of the text. If a document is unpublished, details must be given of the library where it may be seen. Documents which are not available to enquirers must not be referred to, except by 'personal communication'.

Tables should be numbered consecutively using roman numerals and provided with headings.

Mathematical notation should be written with extreme care. Particular care should be taken to differentiate between Greek letters and Roman letters for which they could be mistaken. Double subscripts and superscripts should be avoided, as they are difficult to typeset and read. Notation should be kept as simple as possible. Guidance is given in BS 1991: Part 1: 1976, and *Quantities, Units and Symbols* published by the Royal Society. SI units, or units approved by the World Meteorological Organization, should be used.

Articles for publication and all other communications for the Editor should be addressed to: The Chief Executive, Meteorological Office, London Road, Bracknell, Berkshire RG12 2SZ and marked 'For Meteorological Magazine'.

Illustrations

Diagrams must be drawn clearly, preferably in ink, and should not contain any unnecessary or irrelevant details. Explanatory text should not appear on the diagram itself but in the caption. Captions should be typed on a separate sheet of paper and should, as far as possible, explain the meanings of the diagrams without the reader having to refer to the text. The sequential numbering should correspond with the sequential referrals in the text.

Sharp monochrome photographs on glossy paper are preferred; colour prints are acceptable but the use of colour is at the Editor's discretion.

Copyright

Authors should identify the holder of the copyright for their work when they first submit contributions.

Free copies

Three free copies of the magazine (one for a book review) are provided for authors of articles published in it. Separate offprints for each article are not provided.

Contributions: It is requested that all communications to the Editor and books for review be addressed to the Chief Executive, Meteorological Office, London Road, Bracknell, Berkshire RG12 2SZ, and marked 'For *Meteorological Magazine*'. Contributors are asked to comply with the guidelines given in the *Guide to authors* (above). The responsibility for facts and opinions expressed in the signed articles and letters published in *Meteorological Magazine* rests with their respective authors.

Subscriptions: Annual subscription £36.00 including postage; individual copies £3.25 including postage. Applications for postal subscriptions should be made to HMSO, PO Box 276, London SW8 5DT; subscription enquiries 071–873 8499.

Back numbers: Full-size reprints of Vols 1–75 (1866–1940) are available from Johnson Reprint Co. Ltd, 24–28 Oval Road, London NW1 7DX. Complete volumes of *Meteorological Magazine* commencing with volume 54 are available on microfilm from University Microfilms International, 18 Bedford Row, London WC1R 4EJ. Information on microfiche issues is available from Kraus Microfiche, Rte 100, Milwood, NY 10546, USA.

February 1992

Edited by R.M. Blackall Vol. 121
Editorial Board: R.J. Allam, R. Kershaw, W.H. Moores, P.R.S. Salter No. 1435

Contents

ISSN 0026–1149

ISBN 0-11-728980-9

9 780117 289802

Printed in the United Kingdom for HMSO
Dd 291241 C13 2/92 12521